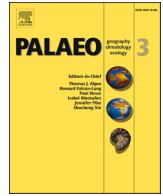




Contents lists available at ScienceDirect

## Palaeogeography, Palaeoclimatology, Palaeoecology

journal homepage: [www.elsevier.com/locate/palaeo](http://www.elsevier.com/locate/palaeo)

# Pollen-based mapping of Holocene vegetation on the Qinghai-Tibetan Plateau in response to climate change

Zhen Li<sup>a</sup>, Yongbo Wang<sup>a,\*</sup>, Ulrike Herzschuh<sup>b,c,d</sup>, Xianyong Cao<sup>e,f</sup>, Jian Ni<sup>g</sup>, Yan Zhao<sup>h</sup>

<sup>a</sup> College of Resource Environment and Tourism, Capital Normal University, Beijing 100048, China

<sup>b</sup> Alfred Wegener Institute Helmholtz Center for Polar and Marine Research, Research Unit Potsdam, Potsdam 14473, Germany

<sup>c</sup> Institute of Environmental Science and Geography, University of Potsdam, Potsdam 14476, Germany

<sup>d</sup> Institute of Biochemistry and Biology, University of Potsdam, Potsdam 14476, Germany

<sup>e</sup> Alpine Paleoeology and Human Adaptation Group (ALPHA), Key Laboratory of Alpine Ecology, Institute of Tibetan Plateau Research, Chinese Academy of Sciences, Beijing 100101, China

<sup>f</sup> CAS Center for Excellence in Tibetan Plateau Earth Sciences, Chinese Academy of Sciences, Beijing 100101, China

<sup>g</sup> College of Chemistry and Life Sciences, Zhejiang Normal University, Jinhua 321004, China

<sup>h</sup> Institute of Geographic Sciences and Natural Resources Research, Chinese Academy of Sciences, Beijing 100101, China

## ARTICLE INFO

Editor: Dr. Howard Falcon-Lang

## Keywords:

Alpine ecosystem  
Fossil pollen record  
Spatial interpolation  
Asian summer monsoon

## ABSTRACT

Improved studies of past vegetation change are required to better understand the variation of alpine ecosystems on the Qinghai-Tibetan Plateau (QTP) in response to future climate change. Spatial and temporal variations of past vegetation can be traced by fossil pollen data mapping. In this paper, we synthesized 57 continuous pollen records on the QTP covering the past 15 kyr to depict large-scale vegetation change and its response to climate variations. In order to minimize potential chronological biases, age-depth models were revised using a state-of-the-art and consistent method for all the records. The spatial and temporal variation of major pollen taxa were examined based on interpolated pollen maps at 1000-year intervals. The arboreal pollen (AP, mainly of *Pinus*, *Betula* and *Abies/Picea*) content expressed significant climate signals over a broad spatial and temporal gradient. During the late glacial period, high proportions of AP widely occurred in regions that are presently unforested owing to the sparse local vegetation coverage. For the Holocene period, AP showed relatively high contributions in records from the southeastern margin of the QTP, with a decreasing gradient in abundance towards the northwest. The transportation of AP to unforested regions corresponds closely to the intensity of monsoon wind, which can be used to track the Holocene evolution of the summer monsoon. The dominant shrub and herbaceous taxa (including *Artemisia*, *Chenopodiaceae*, *Cyperaceae*, *Poaceae* and *Ephedra*) generally represent developments of local vegetation responding to climate variations. In addition, the persistent increase in *Poaceae* pollen during the mid to late Holocene correlates possibly to regional human activities. The inferred spatial and temporal patterns of major pollen types on the QTP provide significant knowledge about long-term vegetation change and its potential response to climate variations.

## 1. Introduction

The Qinghai-Tibetan Plateau (QTP) and its surrounding areas constitute the largest alpine landmass on the Earth, with an average altitude of over 4000 m, which has been informally referred to as the Third Pole on the Earth (Qiu, 2008) and the water tower of the Asian continent (Immerzeel et al., 2020). Consequently, as a driver and amplifier of the climate system, such vast landmass plays an important role in modulating regional and even global climate variations,

particularly the evolution of the Asian Summer/Winter Monsoons and mid-latitude Westerlies (An et al., 2001; Chen et al., 2019; Zhao et al., 2019). Furthermore, climate, vegetation and land surface processes over the QTP reveal extremely sensitive responses to global climate change (Herzschuh et al., 2019; Chen et al., 2020). Therefore, understanding the vegetation and climate change history of the QTP is important to improve our knowledge of large-scale climate patterns as well as their underlying mechanisms. Accordingly, various archives have been investigated during the past decades and interpreted in terms of past

\* Corresponding author.

E-mail address: [yongbowang@cnu.edu.cn](mailto:yongbowang@cnu.edu.cn) (Y. Wang).

<https://doi.org/10.1016/j.palaeo.2021.110412>

Received 3 February 2021; Received in revised form 12 April 2021; Accepted 13 April 2021

Available online 19 April 2021

0031-0182/© 2021 Elsevier B.V. All rights reserved.

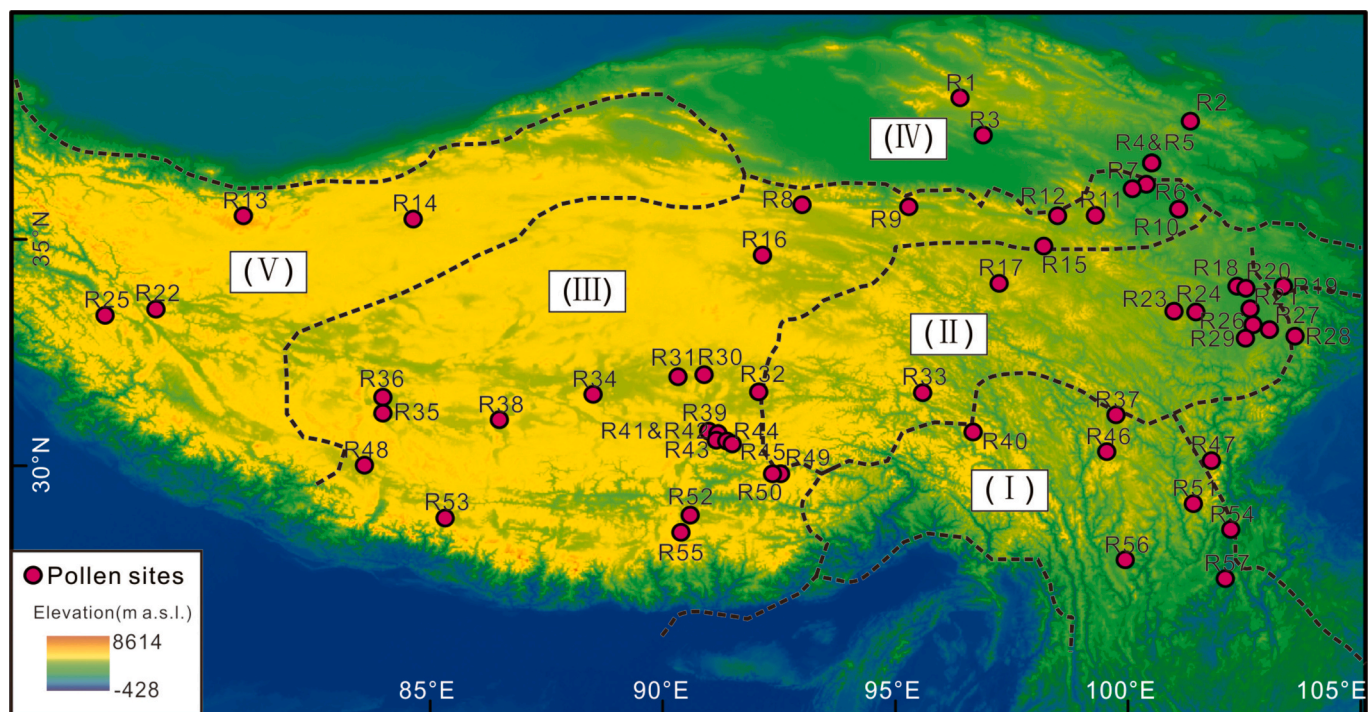


Fig. 1. Distribution of modern vegetation zones on the Qinghai-Tibet Plateau and locations of fossil pollen records (see detailed information in Table 1). For the vegetation zones: I, subalpine conifer forest; II, alpine meadow; III, alpine steppe; IV, temperature desert; V, alpine desert.

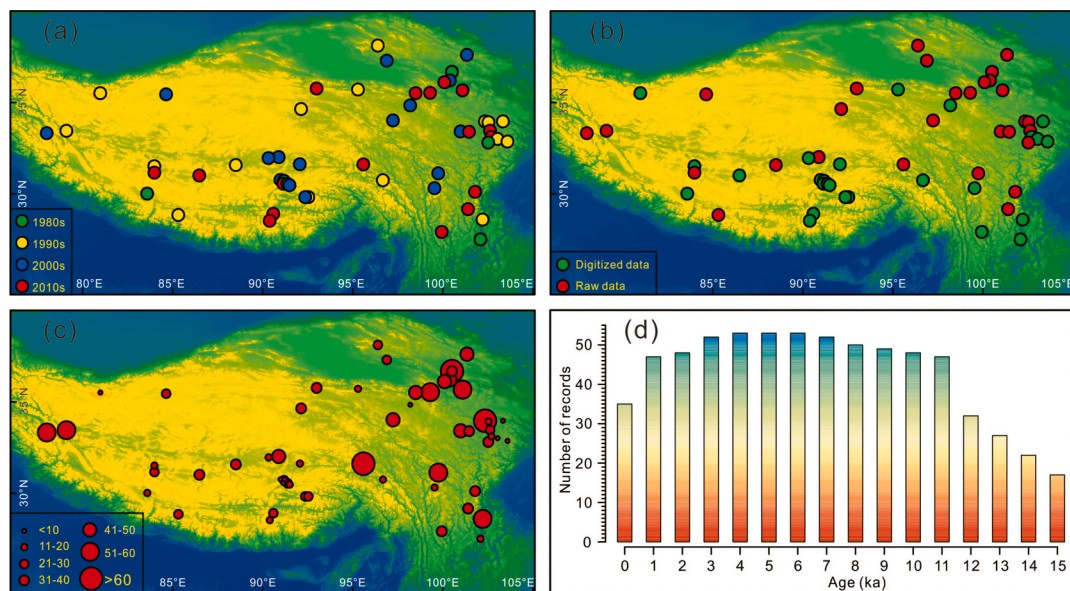


Fig. 2. Overview of the fossil pollen records, (a) publishing time of pollen records, (b) type of data source, (c) number of reported pollen types in each record, and (d) number of available records for each 1000-year slice.

climate fluctuations, for instance, lake sediments (Gasse et al., 1991; Hou et al., 2017a, 2017b), ice cores (Liu et al., 1998; Thompson et al., 1997), stalagmites (Tan et al., 2018) and tree rings (Yang et al., 2014). Among these various paleoclimate proxies, fossil pollen composition makes an especially important contribution owing to its wide distribution and good preservation (e.g., Herzschuh et al., 2019; Hou et al., 2017a, 2017b; Li et al., 2019).

Examining the spatial distribution and temporal variation of vegetation compositions on the QTP is of great significance for understanding alpine vegetation dynamics, underlying driving forces and making predictions for the future. For such a purpose, plenty of fossil pollen

records have been investigated and interpreted since the 1980s (e.g., Wang, 1987; Wang et al., 1981), constituting the overall framework of vegetation history on the QTP (Hou et al., 2017a, 2017b). The combination of individual pollen records will yield further insights concerning regional scale vegetation and climate dynamics. Pollen maps at regional to continental scales were traditionally used to evaluate the late Quaternary vegetation evolution in northeastern North America (Bernabo and Webb III, 1977) and Europe (Huntley and Birks, 1983), which was widely applied following the increase of available fossil pollen data (e.g., Brewer et al., 2017; Gajewski, 2008; Giesecke and Brewer, 2018; Giesecke et al., 2014, 2017; Huntley, 2010; Zanon et al., 2018). Based on

**Table 1**  
Information of fossil pollen records on the Qinghai-Tibet Plateau (see locations in Fig. 1).

| No  | Site Names     | Lat. (°) | Long. (°) | Elev. (m) | Archive type | Type   | No.* dates | Time (ka) | Res.# (yrs) | References                           |
|-----|----------------|----------|-----------|-----------|--------------|--------|------------|-----------|-------------|--------------------------------------|
| R1  | Dunde ice core | 38.10    | 96.40     | 5325      | Ice core     | Raw    | n.d.       | 11.0      | 200         | Liu et al., 1998                     |
| R2  | Lake Luanhaizi | 37.59    | 101.35    | 3200      | Lake         | Raw    | 4          | 26.1      | 500         | Herzschuh et al., 2005               |
| R3  | Lake Hurleg    | 37.28    | 96.90     | 2817      | Lake         | Raw    | 7          | 3–12.5    | 150         | Zhao et al., 2007b                   |
| R4  | Lake Qinghai   | 36.67    | 100.52    | 3200      | Lake         | Raw    | 10         | 18.3      | 70          | Liu et al., 2002                     |
| R5  | Lake Qinghai   | 36.67    | 100.52    | 3200      | Lake         | Raw    | 4          | 11.8      | 350         | Du et al., 1989                      |
| R6  | Lake Dalianhai | 36.20    | 100.40    | 2850      | Lake         | Raw    | 10         | 0–16      | 80          | Cheng et al., 2013                   |
| R7  | Genggahai      | 36.10    | 100.10    | 2860      | Lake         | Raw    | 20         | 0–6.3     | 75          | Huang et al., 2017; Liu et al., 2016 |
| R8  | Lake Kusai     | 35.75    | 93.00     | 4475      | Lake         | Raw    | 7          | 3.6       | 10          | Wang et al., 2012                    |
| R9  | Kunlun-Pass    | 35.70    | 95.30     | 3980      | Profile      | Digit. | 2          | 0–18      | 540         | Liu et al., 1997                     |
| R10 | Xiqing Mount.  | 35.65    | 101.10    | 3780      | Profile      | Raw    | 11         | 1.3–8.2   | 67          | Miao et al., 2015                    |
| R11 | Lake Kuhai     | 35.52    | 99.31     | 4150      | Lake         | Raw    | 13         | 17.5      | 300         | Wischniewski et al., 2011            |
| R12 | Donggi Cona    | 35.50    | 98.50     | 4090      | Lake         | Raw    | 13         | 18.3      | 240         | Wang et al., 2014                    |
| R13 | Sumxi Co       | 35.50    | 81.00     | 5058      | Lake         | Digit. | 6          | 0–12.7    | 80          | van Campo and Gasse, 1993            |
| R14 | Lake Yanghu    | 35.43    | 84.65     | 4778      | Lake         | Raw    | 2          | 12.8      | 700         | Zhao et al., 2007a                   |
| R15 | Ayongwama Co   | 34.83    | 98.20     | 4220      | Lake         | Digit. | 2          | 13.4      | 550         | Cheng et al., 2004                   |
| R16 | Gounong Co     | 34.63    | 92.15     | 4670      | Lake         | Raw    | 3          | 23.1      | 180         | Shan et al., 1996                    |
| R17 | Lake Koucha    | 34.01    | 97.24     | 4540      | Lake         | Raw    | 5          | 15.3      | 230         | Herzschuh et al., 2009               |
| R18 | Zoige RM       | 33.95    | 102.35    | 3400      | Peat         | Raw    | 5          | 8.8       | 180         | Shen et al., 1996                    |
| R19 | Zoige RH       | 33.95    | 103.35    | 3400      | Peat         | Digit. | 3          | 10.8      | 500         | Tang and Shen, 1996                  |
| R20 | Zoige DC       | 33.90    | 102.55    | 3396      | Peat         | Raw    | 1          | 21.1      | 300         | Liu et al., 1995                     |
| R21 | Zoige ZB08     | 33.45    | 102.63    | 3467      | Peat         | Raw    | 9          | 10.3      | 70          | Zhao et al., 2011                    |
| R22 | Bangong Co     | 33.44    | 79.12     | 4300      | Lake         | Raw    | 17         | 10.8      | 270         | van Campo et al., 1996               |
| R23 | Lerzha River   | 33.40    | 101.00    | 4170      | Peat         | Raw    | 3          | 0–10.6    | 480         | Schluetzel and Lehmkuhl, 2009        |
| R24 | Ximen Co       | 33.38    | 101.47    | 4020      | Lake         | Raw    | 17         | 19.8      | 200         | Herzschuh et al., 2014               |
| R25 | Tso Kar        | 33.31    | 78.03     | 4527      | Lake         | Raw    | 32         | 15.1      | 250         | Demske et al., 2009                  |
| R26 | Zoige ZB10     | 33.10    | 102.70    | 3470      | Peat         | Digit. | 20         | 0–10.5    | 50          | Sun et al., 2017                     |
| R27 | Wasong         | 32.99    | 103.05    | 3490      | Peat         | Digit. | 9          | 14.9      | 400         | Yan et al., 1999                     |
| R28 | No. 2 pit      | 32.85    | 103.60    | 3492      | Peat         | Digit. | 9          | 12.7      | 200         | Yan et al., 1999                     |
| R29 | Hongyuan Baihe | 32.80    | 102.53    | 3500      | Peat         | Raw    | 5          | 10.0      | 200         | Wang, 1987                           |
| R30 | Zigetang Co    | 32.00    | 90.90     | 4560      | Lake         | Raw    | 5          | 10.7      | 150         | Herzschuh et al., 2006               |
| R31 | Xuguo Co       | 31.95    | 90.33     | 4595      | Lake         | Digit. | 4          | 8.7       | 170         | Shen, 2003                           |
| R32 | Ahung Co       | 31.62    | 92.07     | 4450      | Lake         | Digit. | 56         | 4.0–9.9   | 50          | Shen, 2003                           |
| R33 | Butuo Co       | 31.60    | 95.60     | 4682      | Lake         | Raw    | 3          | 0–11.1    | 155         | Zhang et al., 2015                   |
| R34 | Selin Co       | 31.57    | 88.52     | 4530      | Lake         | Raw    | 5          | 13.3      | 250         | Sun et al., 1993                     |
| R35 | Lake Zabuye    | 31.50    | 84.00     | 4420      | Lake         | Digit. | 3          | 27.1      | 1500        | Wu and Xiao, 1996                    |
| R36 | Taro Co        | 31.15    | 84.00     | 4566      | Lake         | Raw    | 12         | 10.2      | 150         | Ma et al., 2014                      |
| R37 | Lake Naleng    | 31.11    | 99.76     | 4200      | Lake         | Raw    | 16         | 16.4      | 80          | Kramer et al., 2010a, 2010b          |
| R38 | Tangra Yumco   | 31.00    | 86.50     | 4545      | Lake         | Digit. | 28         | 3–17.5    | 115         | Ma et al., 2019a, 2019b              |
| R39 | Nam Co         | 30.75    | 91.00     | 4718      | Lake         | Digit. | 3          | 7.6       | 300         | Herrmann et al., 2010                |
| R40 | Ren Co         | 30.73    | 96.68     | 4450      | Lake         | Digit. | 7          | 17.0      | 400         | Tang et al., 1999                    |
| R41 | Dangxiong-8    | 30.70    | 91.20     | 4370      | Peat         | Digit. | 3          | 0–10      | 475         | Wang et al., 1981.                   |
| R42 | Dangxiong-9    | 30.70    | 91.20     | 4270      | Peat         | Digit. | 3          | 0–10      | 500         | Wang et al., 1981.                   |
| R43 | Cuo Na         | 30.55    | 91.16     | 4515      | Wetland      | Digit. | 7          | 8.5       | 140         | Cheng et al., 2014                   |
| R44 | Wumaqu         | 30.53    | 91.38     | 4370      | Peat         | Raw    | 3          | 12.0      | 600         | Wang et al., 1988                    |
| R45 | Ngion Co       | 30.47    | 91.50     | 4515      | Lake         | Digit. | 12         | 5.9       | 100         | Shen et al., 2008                    |
| R46 | Lake Yidun     | 30.30    | 99.55     | 4470      | Lake         | Digit. | 3          | 13.8      | 400         | Shen et al., 2006                    |
| R47 | Muge Co        | 30.10    | 101.80    | 3780      | Lake         | Raw    | 8          | 0–12      | 64          | Ni et al., 2019                      |
| R48 | Dawalong       | 30.00    | 83.60     | 4570      | Peat         | Digit. | 4          | 0–10      | 400         | Wang et al., 1981                    |
| R49 | Lake Hidden    | 29.81    | 92.54     | 4980      | Lake         | Digit. | 3          | 13.5      | 500         | Tang et al., 1999                    |
| R50 | Qongjiemong    | 29.81    | 92.37     | 4980      | Lake         | Digit. | 22         | 14.0      | 200         | Shen, 2003                           |
| R51 | Lake Wuxu      | 29.15    | 101.41    | 3705      | Lake         | Raw    | 18         | 11.9      | 40          | Zhang et al., 2016                   |
| R52 | Chen Co        | 28.90    | 90.60     | 4420      | Lake         | Digit. | 6          | 2.6–10    | 120         | Lu et al., 2011                      |
| R53 | Peiku Co       | 28.83    | 85.33     | 4590      | Lake         | Raw    | 3          | 5–14.7    | 100         | Huang, 2000                          |
| R54 | Lake Shayema   | 28.58    | 102.22    | 2400      | Lake         | Digit. | 5          | 11.9      | 130         | Jarvis, 1993                         |
| R55 | Pumoyum Co     | 28.52    | 90.40     | 5010.     | Lake         | Digit. | 60         | 3–15.1    | 160         | Nishimura et al., 2014               |
| R56 | Lake Shudu     | 27.91    | 99.95     | 3630      | Lake         | Digit. | 3          | 11–17.1   | 500         | Cook et al., 2011                    |
| R57 | Lake Dahaizi   | 27.5     | 102.1     | 3660      | Lake         | Digit. | 3          | 0–12.4    | 2500        | Li and Liu, 1988                     |

No. \*, number of dating controls; Res. #, temporal resolution of fossil pollen data.

the fossil pollen records from China, Holocene pollen maps were constructed and interpreted along with vegetation changes (Ren and Beug, 1999, 2002; Ren and Zhang, 1998), focusing mainly on the northeastern and northern parts of China. A more comprehensive synthesis study revealed the spatial and temporal distributions of major tree taxa in eastern Asia continent over the past 22,000 years (Cao et al., 2014), while vegetation maps for southern China was conducted recently at selected time slices (Wang et al., 2019). However, restricted by the spatial extents of previous studies, regional vegetation and potential climate patterns were not captured for the QTP region. In particular, recent investigations of modern pollen depositions on the plateau revealed close correlations between spatial variation of exotic pollen (i.

e., arboreal taxa) and the intensity/flow path of Asian Summer Monsoon, pointing out potential applications of fossil pollen records beyond the traditional reconstructions of region vegetation and climate evolution histories (Li et al., 2020; Zhang and Li, 2017). However, the question that whether such hypothesis could be verified and applied to fossil pollen records is still open.

Many fossil pollen records are available from the QTP covering the period since the late glacial, which focus mainly on the vegetation and/or climate inferences concerning individual sampling site or limited spatial scales. So far, whether these fossil pollen compositions exhibit large scale patterns corresponding to climate fluctuations or rather local peculiarities is not yet fully understood. In this study, 57 fossil pollen

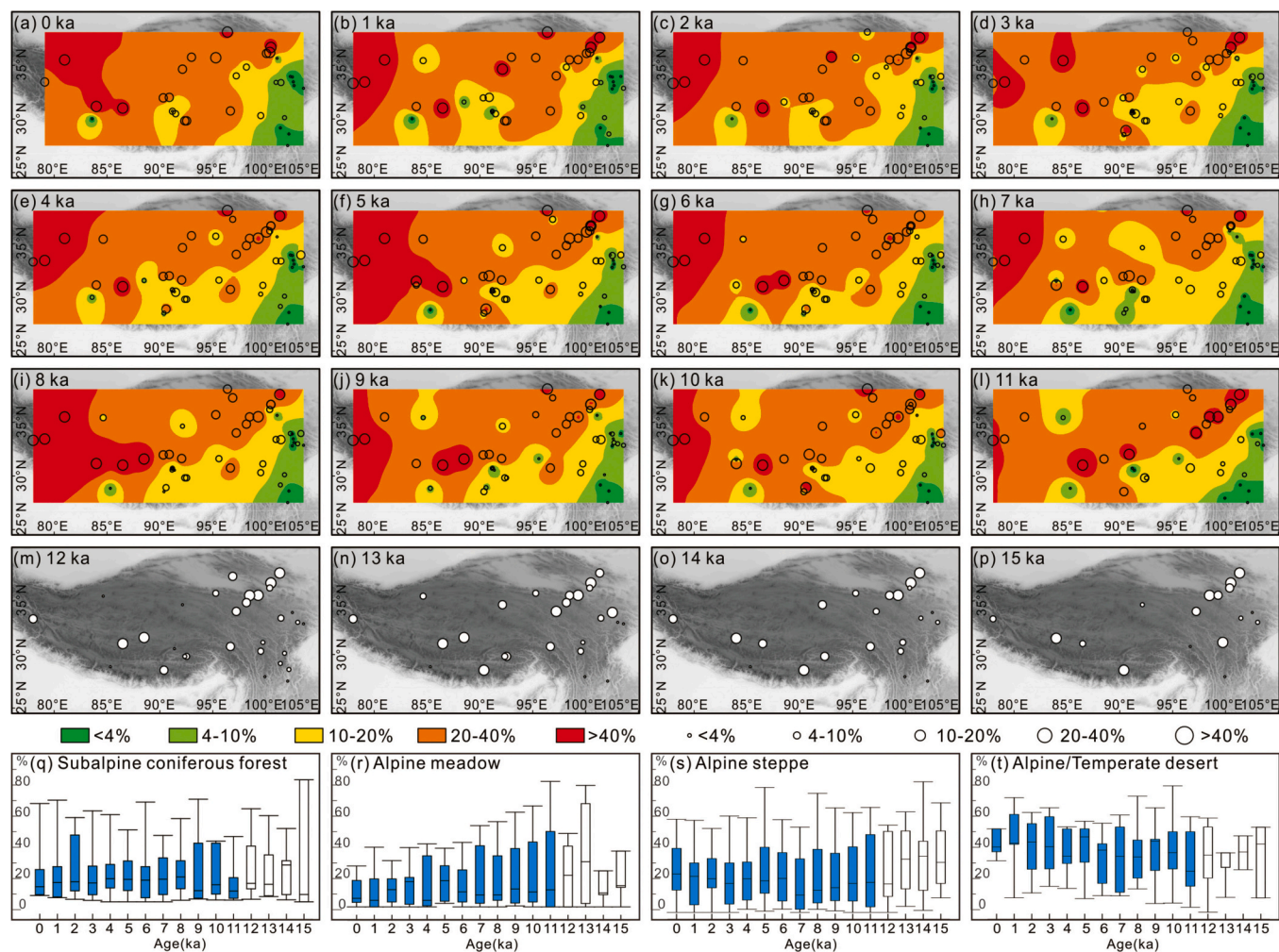


**Fig. 3.** Variation of *Artemisia* content in each record (open circles) and spatial interpolations (colored shades) at 1000-year interval for the last 15 kyr (a-p). The boxplots indicate the variation ranges of *Artemisia* from four vegetation zones (q-t). The time period between 15 and 12 ka were not interpolated owing the limited number of records, which were indicted as open boxes as well.

records covering the past 15,000 years were collected and synthesized. Interpolated maps at 1000-year interval were established for major pollen types, with specific focuses on (1) representing the large scale spatial and temporal patterns of vegetation change on the QTP since the late glacial, (2) revealing the potential climate inferences from the vegetation history, and (3) examining the variation of arboreal pollen as an indicator for the Asian Summer Monsoon (ASM) evolution.

## 2. Study area

The Qinghai-Tibetan Plateau (QTP, 26°00'-39°47'N, 73°19'-104°47'E), with an area of over 2.3 million km<sup>2</sup>, receives complex influences from the Indian Summer Monsoon (ISM), the East Asian Summer Monsoon (EASM), and the mid-latitude Westerlies (Chen et al., 2020). Accordingly, mean annual temperature of the QTP decreases from approximate 20 °C in the southeast to below -6 °C in the northwest. As the warm and humid air flows during the monsoon season from the oceans are blocked by the high mountains, an obvious gradient in mean annual precipitation shows decreasing trend from 2000 mm in the southeastern margin to less than 50 mm in the central and northwestern plateau (Sun, 1999).

Following the climate gradient, modern vegetation on the QTP is characterized by an obvious zonal distribution, from subtropical forest/subalpine conifer forest in the southeastern margin, to alpine shrub, alpine meadow, alpine steppe and alpine desert towards the

northwestern QTP (Chang, 1983; Hou, 2001; Fig. 1). Subalpine coniferous forests (mainly of *Abies* and *Picea*) with mixture of *Rhododendron* are found on southeastern and eastern margins. The southeastern part of the plateau is covered by subalpine shrublands (e.g., *Salix*, *Potentilla*, *Rhododendron*, *Lonicera*, *Caragana* and *Berberis*) and alpine meadows consisting of various *Kobresia* species, such as *K. pygmaea*, *K. humilis*, and *K. capillifolia*, together with limited abundances of Poaceae plants (e.g., *Stipa purpurea*), *Artemisia* (e.g., *A. gmelinii*, *A. argyi*) and Chenopodiaceae (e.g., *Chenopodium hybridum*). The central part of the plateau comprises alpine steppes dominated by a mixture of plant species from Cyperaceae (e.g., *Kobresia littledalei*, *K. royleana*, *Carex moorcroftii*), Poaceae (*Stipa subsessiliflora*, *S. purpurea*) and *Artemisia* (e.g., *A. salsoloides*). Alpine deserts develop in the northwestern part of the plateau owing to the limited moisture, which is dominated by Chenopodiaceae species (e.g., *Ceratoides compacta*) accompanied by *Artemisia* (*A. frigida*, *A. salsoloides*), Poaceae (e.g., *Stipa subsessiliflora*, *S. purpurea*, *S. glareosa*), *Ephedra* (*E. przewalskii*) and *Nitraria* (*N. roborowskii*, *N. sibirica*). Temperate desert and steppe vegetations are also distributed on the northern margin of the plateau and the Qaidam Basin where elevations are slightly low (Wang et al., 2006; Wu, 1995).

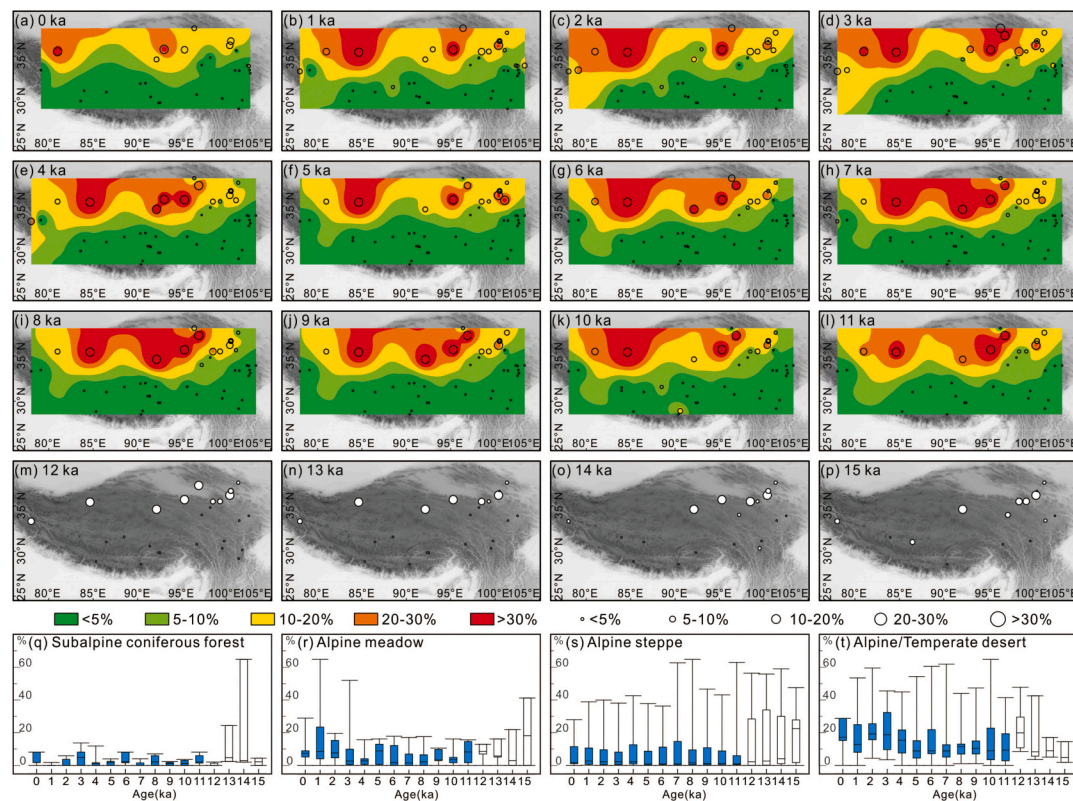


**Fig. 4.** Variation of Chenopodiaceae content in each record (open circles) and spatial interpolations (colored shades) at 1000-year interval for the last 15 kyr (a-p). The boxplots indicate the variation ranges of Chenopodiaceae from four vegetation zones (q-t). The time period between 15 and 12 ka were not interpolated owing to the limited number of records, which were indicated as open boxes as well.

### 3. Data and methods

#### 3.1. Collection of fossil pollen records

Fossil pollen records were collected from the Qinghai-Tibetan Plateau (QTP) and surrounding area with an elevation of over 3000 m, which should meet the following criteria (1) the record should continuously cover at least 4000 years during the past 15 kyr (thousands of years), (2) the temporal resolution of the pollen record should be higher than 500 years, and (3) the chronology should be established based on at least 3 dating results. Nevertheless, restricted by the spatial distribution of available data, a few records with slightly lower temporal resolution or fewer dating controls were included in the dataset (for example, Lake Zabuye, Wu and Xiao, 1996; Lake Yanghu, Zhao et al., 2007a, in order to achieve a more comprehensive spatial pattern of the pollen compositions.

#### 3.2. Recalibration of radiocarbon ages

The chronology of all the records (except one ice core record) is based on radiocarbon dates, which are available from the original publications. In most cases, the radiocarbon dates were calibrated and interpolated, however, which were accomplished based on various interpolation methods and calibration databases. For the purpose towards a consistent calibration of all radiocarbon dates, we have constructed new age-depth models for all the records using the Bayesian method (Bacon, Blaauw and Christen, 2011), which takes the accumulation rates in lakes or peats into account and has been widely applied in palaeoecological studies. The calibrations were accomplished by the Bacon v2.2 package using the IntCal13 dataset, which was performed in

R 3.5.2 program (Reimer et al., 2013; R Development Core Team 2013). In addition, as widely reported from Tibetan lakes, the influence of carbon reservoir effect on radiocarbon dates was corrected prior to the calibrations according to the descriptions in original publications (Hou et al., 2012; Mischke et al., 2013). Subsequently, chronology of the collected fossil pollen records was re-established and interpolated.

#### 3.3. Interpolation of major pollen taxa

In order to illustrate the temporal and spatial patterns of vegetation change on the QTP, pollen distribution maps at 1000-year interval since 15 ka were conducted in ArcMap v10.2 through spatial interpolation of pollen compositional data. Inverse distance weighting (IDW) method provided in Spatial Analysis Tools was applied with a five-scale classification for each taxon according to individual percentage range. Due to the uneven temporal resolution of pollen data, samples within a window of  $\pm 300$  years was selected to represent the pollen composition at each time slice and used for the spatial interpolations (Brewer et al., 2017). In total, pollen data from eight taxa were selected for mapping, consisting of three arboreal taxa (*Pinus*, *Betula* and *Abies/Picea*) and five herbaceous/shrub taxa (*Artemisia*, Chenopodiaceae, Poaceae, Cyperaceae and *Ephedra*), which expressed high contributions in both fossil pollen assemblages and modern vegetation compositions, representing the most common plant types in the study area (Ren and Beug, 2002). The sum of arboreal pollen content (AP) and *Artemisia*/Chenopodiaceae ratio (A/C) were also included in the analysis considering their extensive applications. In addition, pollen proportion data from 15 to 12 ka were presented without interpolations owing to the limited number of records and heterogeneous spatial distributions (Fig. 2d).

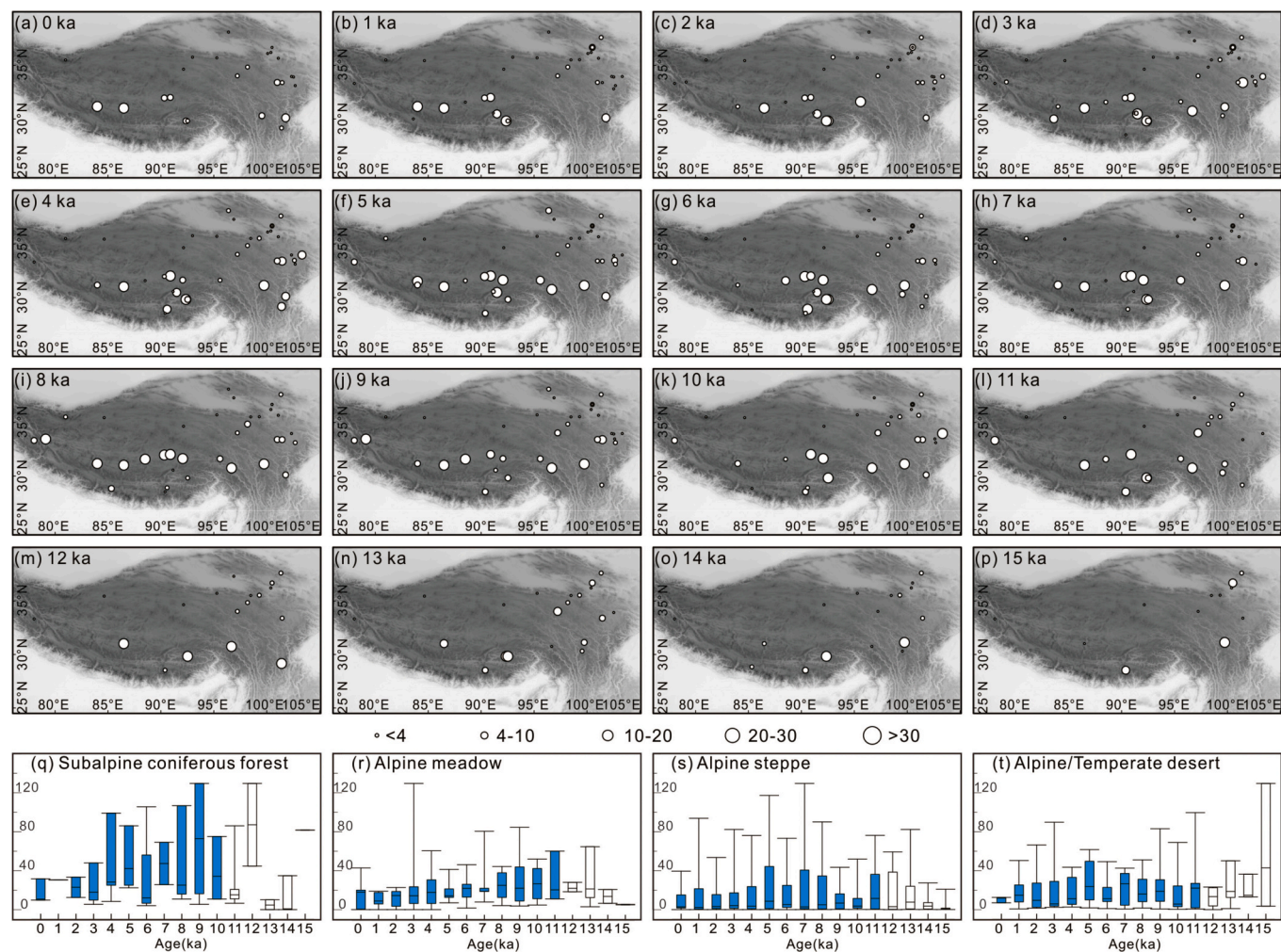


**Fig. 5.** Variation of *Artemisia*/Chenopodiaceae ratio in each record (open circles) at 1000-year interval for the last 15 kyr (a-p). The boxplots indicate the variation ranges of *Artemisia*/Chenopodiaceae ratio from four vegetation zones (q-t). The time period between 15 and 12 ka were indicated as open boxes owing the limited number of records.

## 4. Results

### 4.1. Overview of selected pollen records and interpolation maps

In total, 57 fossil pollen records were collected and synthesized, consisting of records presented in Cao et al. (2013) and recent publications (see locations in Fig. 1 and detailed information in Table 1). Pollen records were collected from all the vegetation zones, despite the fact that more records were distributed in eastern and southern parts of the plateau (Fig. 1). Generally, most data were published in the past two decades, together with 7 records reported in the 1980s (Fig. 2a). Meanwhile, the pollen data were mainly retrieved from continuous archives, including sediments from 39 lake cores and 13 peat sequences, 1 ice core record (i.e., Dunde; Liu et al., 1998), as well as a few records from profiles and swamps (Table 1). Raw pollen data were inferred for 31 records, which were either provided by the authors or available from publications, while pollen compositional data for the remaining 26 records were digitized from published pollen diagrams (Fig. 2b; Cao et al., 2013). Generally, more than 20 pollen types were reported in most records, which reached up to over 60 species in recently published records (Fig. 2c). In addition, the number of available pollen records at different time slices shows stable values around 50 during the Holocene, with slightly fewer records for the period before 12 ka (Fig. 2d).

The interpolation maps of each taxon represent their spatial distribution and temporal variations at 1000-year interval, revealing the

spatial and temporal patterns of regional vegetation compositions on the QTP. For the arboreal taxa, *Pinus* shows generally higher values (ca. 40%) as well as wider distributions, while the distributions of *Betula* and *Abies/Picea* are mainly restricted to the eastern/southeastern parts of the plateau. As the dominant components in most records, herbaceous taxa of *Artemisia*, Chenopodiaceae, Poaceae and Cyperaceae showed high proportions, while *Ephedra* contributed only limited content under 10%.

### 4.2. Temporal and spatial variations of major pollen taxa during the past 15 kyr

According to the synthesis and interpolation of fossil pollen records, the spatial and temporal variations of the typical pollen taxa on the QTP since 15 ka are summarized as follows.

#### 4.2.1. *Artemisia*

the proportion of *Artemisia* decreases gradually from the northwestern part of the plateau to the southeastern margin (Fig. 3). Records with *Artemisia* content of over 40% are mainly distributed in the northwestern plateau, for instance, Tso Kar, Bangong Co and Sumxi Co, corresponding to the area currently dominated by alpine desert communities. On the other hand, the contribution of *Artemisia* in total pollen composition is generally less than 10% for the records retrieved from southeastern margin of the plateau (e.g., Lake Wuxu, Muge Co), as the mountainous region is mainly covered by subalpine conifer forest or

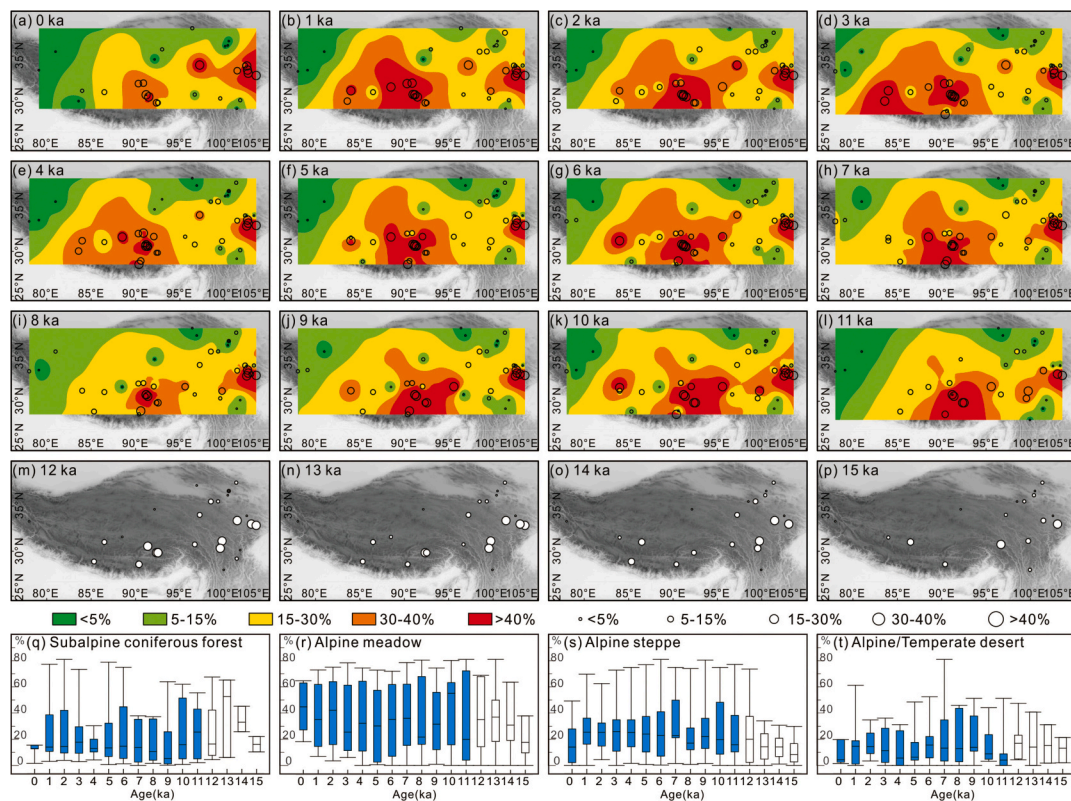


**Fig. 6.** Variation of Cyperaceae content in each record (open circles) and spatial interpolations (colored shades) at 1000-year interval for the last 15 kyr (a-p). The boxplots indicate the variation ranges of Cyperaceae from four vegetation zones (q-t). The time period between 15 and 12 ka were not interpolated owing the limited number of records, which were indicated as open boxes as well.

subtropical forest. For the records collected from central QTP where alpine steppe and alpine meadow communities develop, moderate contents of *Artemisia* ranging between 10% and 40% were commonly reported, for instance, Lake Kusai, Ayongwama Co. Temporally, *Artemisia* occupied relatively low and stable contents in the forest area (around 10%), with slightly higher proportions before 8 ka and a gradual decrease afterwards (Fig. 3q). For records from alpine meadow (average of ca. 20%) and alpine steppe (average up to 40%) areas, the variation of *Artemisia* expressed roughly consistent patterns, with relatively higher compositions between 11 and 8 ka followed by a gradually decline after 7 ka (Fig. 3r, s). On the other hand, the content of *Artemisia* in the desert area decreased slightly during the early Holocene between 11 and 8 ka, and increased progressively after 7 ka (Fig. 3t).

#### 4.2.2. *Chenopodiaceae*

*Chenopodiaceae* pollen is widely identified showing high proportions in sites from the northern QTP and Qaidam Basin, corresponding to the distribution of alpine desert and temperate desert vegetation zones respectively (Fig. 4). Meanwhile, consistent spatial patterns illustrating a southward decline of *Chenopodiaceae* pollen content were determined across the time slices. Dominant compositions of *Chenopodiaceae* (over 30% in total pollen assemblage) were reported in records from the present desert area, for instance, Lake Yanghu, Kunlun Pass profile. Moderate content of *Chenopodiaceae* was found in records from the alpine steppe and alpine meadow zones, which decreases along with the increasing distance away from the deserts. Only minor portions of *Chenopodiaceae* pollen were detected from records in the southeastern margin of QTP, which are predominantly less than 2%, except slightly higher values at 13 and 14 ka detected from Lake Yidun (3% and 8%, respectively; Fig. 4q). The content of *Chenopodiaceae* in the alpine meadow zone was generally less than 10%, expressing a slightly increasing trend after 7 ka (Fig. 4r). High proportions of

*Chenopodiaceae* were recovered from the alpine steppe zone before the Holocene, even though available from limited records, which could reach up to 30%, such as samples from Gounong Co. The content was relatively stable during the first half of the Holocene followed by an increasing trend after 6 ka (Fig. 4s). In the desert areas, *Chenopodiaceae* content decreased from 11 ka to 7 ka, which was followed by a persistent increase after 7 ka (Fig. 4t).

#### 4.2.3. *Artemisia/Chenopodiaceae* ratio

according to the variations of *Artemisia* and *Chenopodiaceae*, the A/C ratio expressed clear spatial patterns as well (Fig. 5). High values (over 30) were reported from the subalpine forest and alpine steppe zones, despite that the ratio should be treated with caution in the forest zone owing to the limited abundances of these two types plants (Fig. 5q). The A/C ratios from alpine meadow and the deserts are relatively low (ca. 20), which expressed overall consistent temporal patterns as subalpine forest and alpine steppe zones (Figs. 5r, t). Generally, the A/C ratios were relatively high during the early Holocene, and decreased gradually after 5 ka.

#### 4.2.4. *Cyperaceae*

Records with high *Cyperaceae* contents were distributed mainly in the southern and eastern parts of the plateau, with values of over 40% in the total pollen assemblage, corresponding to the alpine meadow and the transitional zone from alpine meadow to alpine steppe, such as Nam Co and No.2 pit (Fig. 6). In the desert areas from northwestern and northeastern parts of the plateau, *Cyperaceae* content was generally less than 15%, such as Sumxi Co and Lake Hurleg. In the subalpine coniferous forest vegetation zone on the southeastern plateau, *Cyperaceae* content show fluctuant compositions among records ranging from 5% up to 80% (Fig. 6q). Meanwhile, relatively low contents were recovered in the early-mid Holocene period, which increased slightly after 6 ka

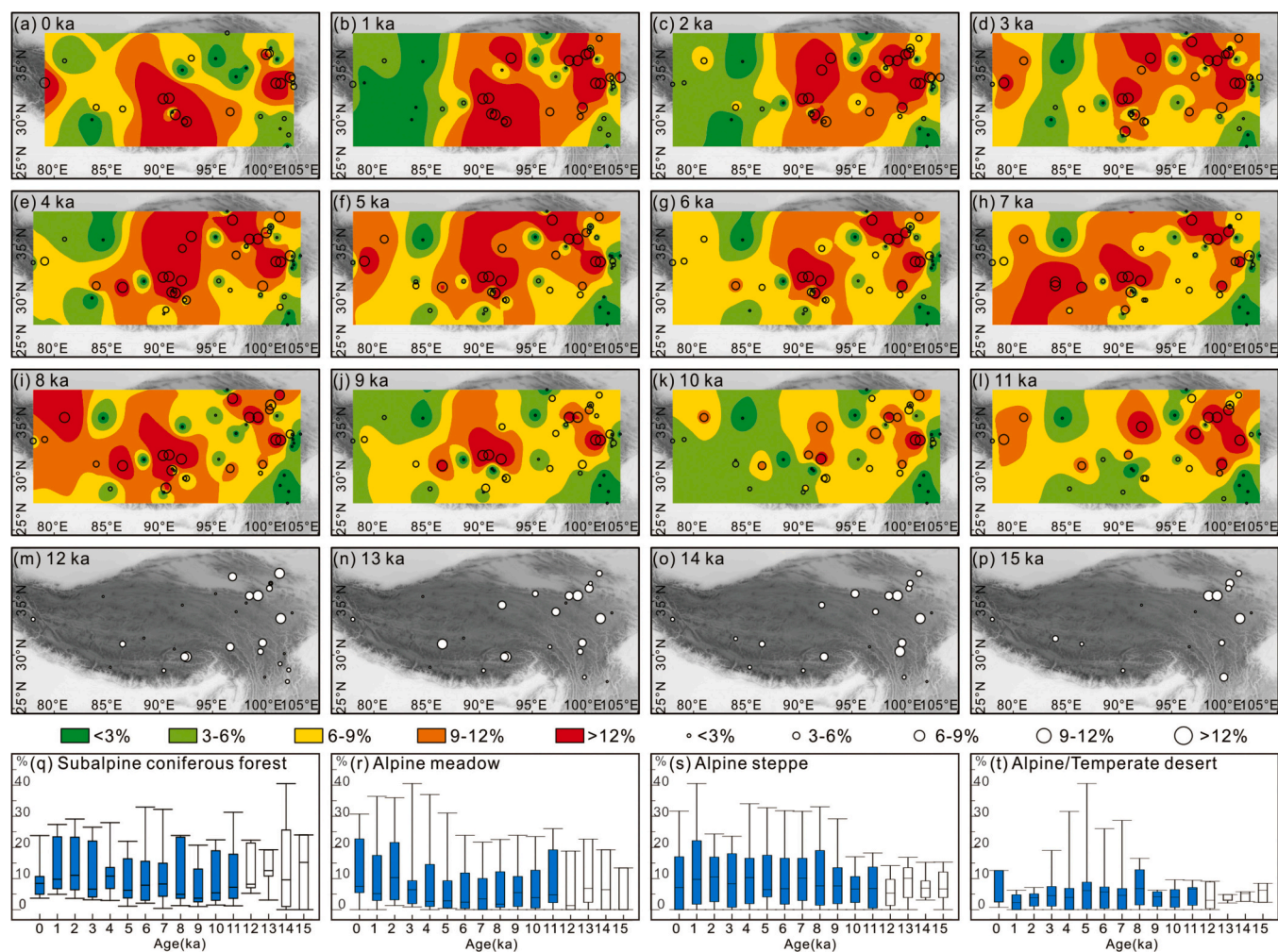


Fig. 7. Variation of Poaceae content in each record (open circles) and spatial interpolations (colored shades) at 1000-year interval for the last 15 kyr (a-p). The boxplots indicate the variation ranges of Poaceae from four vegetation zones (q-t). The time period between 15 and 12 ka were not interpolated owing the limited number of records, which were indicted as open boxes as well.

(Fig. 6q). For the alpine meadow, contribution of Cyperaceae to the total pollen assemblages can reach as high as 80%, which expressed a rather stable pattern with minor fluctuations (Fig. 6r). Except for different levels of Cyperaceae content in alpine steppe (approximately 40%, Fig. 6s) and the deserts (below 25%, Fig. 6t), temporal variation trends are briefly consistent, illustrating gradual increases from 11 to 8 ka and progressive declines afterwards.

#### 4.2.5. Poaceae

Poaceae pollen is widely distributed on the plateau, while records showing high values are mainly concentrated in the northeastern part (Fig. 7). Moderate contents of Poaceae (ca. 15%) were reported from records in the subalpine forest areas, which shows a gradual increasing trend after 7 ka (Fig. 7q). In the alpine meadow zone, Poaceae content was about 10% in the total pollen assemblage, which decreased gradually from 11 to 8 ka, and then increased slightly after 8 ka (Fig. 7r). In the alpine steppe area, the content was rather low in the pre-Holocene stage and became higher after entering the Holocene (Fig. 7s). The Poaceae content in desert areas were mostly below 10%, together with high content in some time slices, such as high content reaching about 40% from Lake Hurleg between 7 and 4 ka (Fig. 7t). In addition, a progressive increasing trend after 7 ka could be detected for Poaceae, except for the last 3000 years in the desert area.

#### 4.2.6. Ephedra

The spatial distribution of *Ephedra* on the plateau is similar to Chenopodiaceae, with much lower proportions in the records (Fig. 8). Generally, two distribution centers could be identified in the northern plateau, with content of *Ephedra* over 10%, such as Lake Yanghu and Kunlun Pass section. The content was at a moderate level in alpine steppe and alpine meadow area in the central part of plateau, ranging from 3% to 5%, such as Lake Koucha and Ayongwama Co. The pollen of *Ephedra* was merely identified from the subalpine coniferous forest area in the southeastern margin, e.g., Lake Naleng (Fig. 8q). In the alpine meadow zone, the content of *Ephedra* was slightly higher before the Holocene, which was generally lower than 5% in the Holocene period (Fig. 8r). The temporal variations of *Ephedra* in the steppe and desert zones were generally consistent. The content increased gradually during the late Glacial and reached the maxima at the Holocene transition period, which decreased slightly until 7 ka and followed by a gradually increase afterwards (Fig. 8s, t).

#### 4.2.7. Betula

From southeastern to northwestern parts of the plateau, the proportion of *Betula* decreased gradually (Fig. 9). In the subalpine coniferous forest area on the southeastern margin of the plateau, the content was briefly greater than 15% in each individual time slice, such as Lake Naleng and Lake Yidun. Extremely low values (less than 1%) were found in the alpine desert records from the northwestern plateau, for instance,



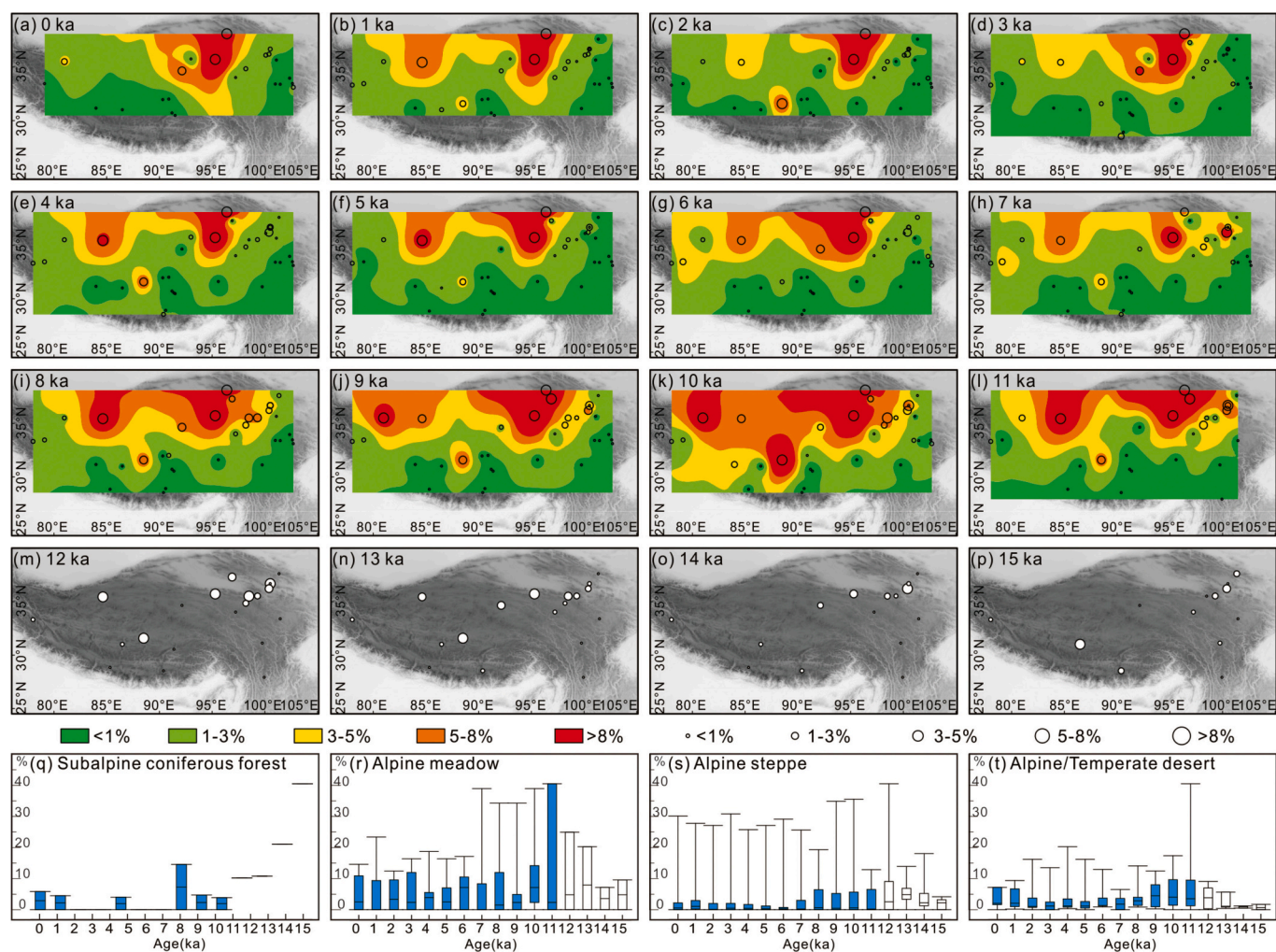


**Fig. 8.** Variation of *Ephedra* content in each record (open circles) and spatial interpolations (colored shades) at 1000-year interval for the last 15 kyr (a-p). The boxplots indicate the variation ranges of *Ephedra* from four vegetation zones (q-t). The time period between 15 and 12 kyr were not interpolated owing the limited number of records, which were indicated as open boxes as well.

Bangong Co and Lake Yanghu. The content of *Betula* shows major variations ranging from 5% to 8% in records from alpine meadow (e.g., Lerzha River section and Ximen Co), and 1–5% in alpine steppe (e.g., Chen Co and Ahung Co). In the subalpine coniferous forest area, the content of *Betula* was relatively low before Holocene, which increased abruptly up to 30% after entering the Holocene, and decreased gradually since 7 ka (Fig. 9q). The temporal variations in alpine meadow and alpine steppe zones reveal broadly consistent patterns, showing low values before Holocene, high content during the early Holocene and gradual declines after 5 ka (Fig. 9r, s). The overall content of *Betula* in desert area was even higher than the records from alpine meadow and alpine steppe, particularly the high contributions of nearly 15% before 9 ka (Fig. 9t). The content decreased gradually after 9 ka, and reached a relatively stable condition after 5 ka with a slightly increasing trend (Fig. 9t).

#### 4.2.8. *Pinus*

Compared to *Betula*, the distribution of *Pinus* pollen expresses a much wider range on the plateau, together with higher contributions in each individual record (Fig. 10). For the mountainous region covered by subalpine coniferous forests on the southeastern edge, the content of *Pinus* can reach up to nearly 40%, such as Lake Shayema and Lake Dahaizi. In the central part of plateau where alpine steppe and alpine meadow develop today, the overall *Pinus* content is between 2% and 10% (Lake Zigetang and sections from Zoige Basin), while in the desert

areas in the northwest, such as Lake Yanghu and Bangong Co, *Pinus* content is much lower. Temporally, the content of *Pinus* in the forest areas was relatively high (about 40%) along with minor fluctuations that no obvious trend of change could be deduced (Fig. 10q). The content of *Pinus* varies broadly among records at each time slice in the alpine meadow area, ranging between 10% and over 50% at certain sites (Fig. 10r). Large scale fluctuations of *Pinus* were also revealed in records from steppe and desert areas, with relatively high proportions during the last 4000 years in steppe area, and between 7 and 4 ka in the desert area, respectively (Fig. 10s, t).

#### 4.2.9. *Abies/Picea*

The distribution of *Abies/Picea* is mainly concentrated in the Zoige Basin of eastern QTP, which is slightly different from *Betula* and *Pinus* (Fig. 11). The content of *Abies/Picea* can reach over 40% in the alpine meadow zone, mainly in the records from Zoige Basin, e.g., Zoige DC, Zoige RH and Hongyuan Baihe. Meanwhile, in the subalpine forest areas covered by broad-leaved and coniferous forests in the southeastern margin of the plateau, the content of *Abies/Picea* is around 20%, for example, Lake Shayema and Lake Dahaizi. The composition of *Abies/Picea* is extremely low in alpine steppe and desert regions, with median values around 1% in most of the records. The content of *Abies/Picea* in the forest area was relatively stable throughout the whole period, with slightly higher values at 8 ka and 9 ka from Ren Co and Lake Yidun (Fig. 11q). Generally, high contributions of *Abies/Picea* were reported

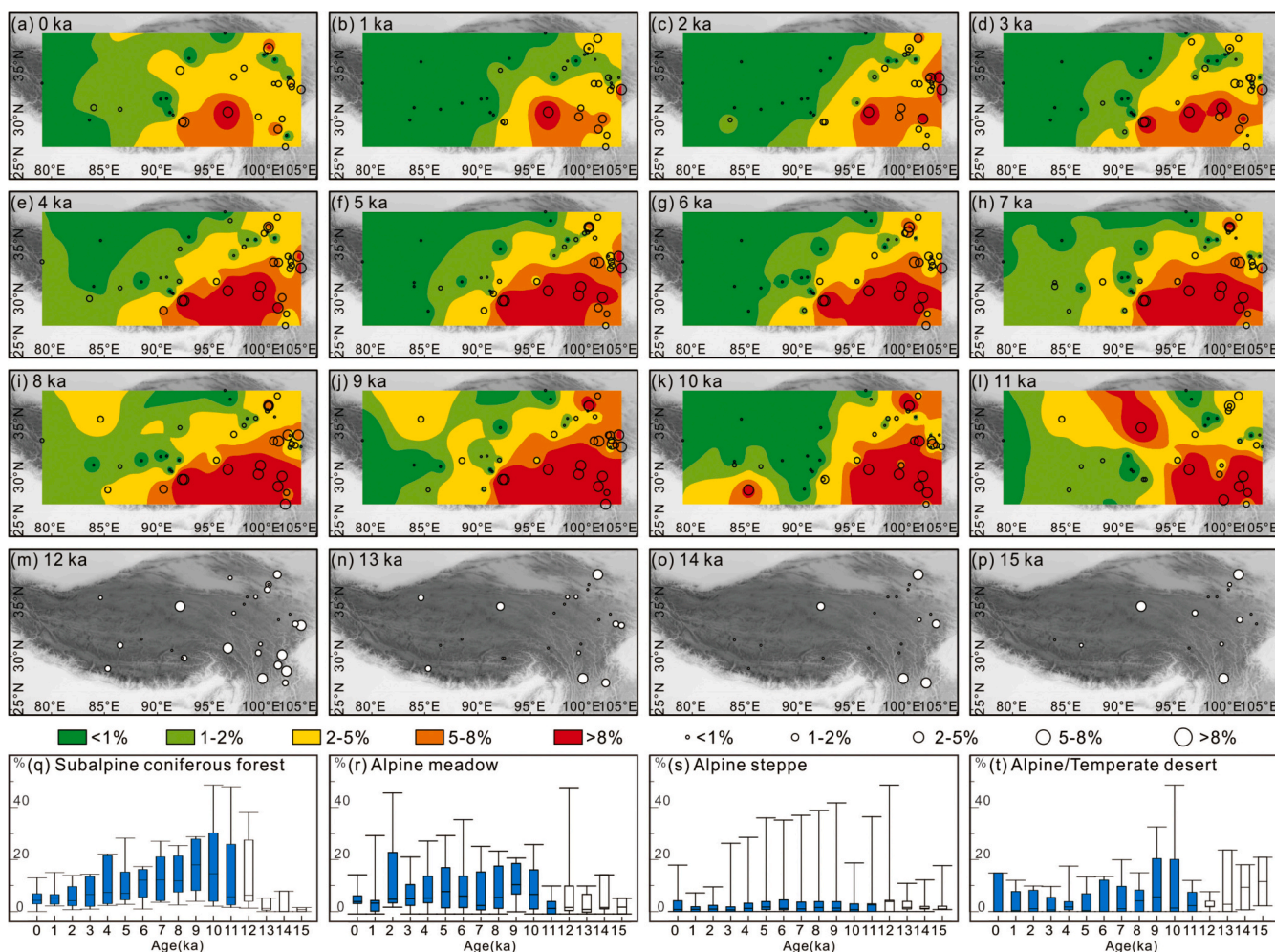


**Fig. 9.** Variation of *Betula* content in each record (open circles) and spatial interpolations (colored shades) at 1000-year interval for the last 15 kyr (a-p). The boxplots indicate the variation ranges of *Betula* from four vegetation zones (q-t). The time period between 15 and 12 ka were not interpolated owing the limited number of records, which were indicted as open boxes as well.

from alpine meadow with values over 60%, which showed relatively high levels between 11 and 7 ka and a gradual decrease after 7 ka (Fig. 11r). Roughly stepwise declines of *Abies/Picea* content could be noticed throughout the records in alpine steppe and desert zones (Figs. 11 s, 11 t).

#### 4.2.10. Arboreal Pollen (AP)

High proportions of arboreal pollen (AP, over 40%) is mainly distributed in the mountainous region of eastern and southeastern plateau, which decreases gradually towards northwest (Fig. 12). AP showed moderate contributions in records from alpine steppe and alpine meadow, while its content in the records from alpine desert (i.e., northwestern plateau) are briefly less than 4%, e.g., Sumxi Co and Bangong Co. Considering the extremely high over-representation and dispersal ability of *Pinus* pollen, spatial and temporal patterns of *Pinus*-excluded arboreal pollen (PeAP) on the plateau were examined as well, which reveals a more obvious spatial gradient (Fig. 13). In addition, area with high PeAP content occupied the southeastern margin of the plateau, which expanded progressively during the early to mid-Holocene and retreated after 6 ka (Fig. 13). Despite slight differences in the percentage values between AP and PeAP, the temporal variation patterns were highly consistent. High values dominate the first half of the records before 7 ka, while a decreasing trend dominated the rest part of Holocene, except for minor increases in records from the deserts after 3 ka (Figs. 12, 13).

## 5. Discussion

### 5.1. Potential uncertainties in source data

Although necessary site selection as well as data quality control have been processed, potential uncertainties may have also arisen from the following aspects.

#### 5.1.1. Dating uncertainties

the chronology of almost all the records were established based on radiocarbon dates, for which necessary corrections and re-calibrations have been performed to reduce the potential biases. However, the influence of carbon reservoir effect (Hou et al., 2012), especially its unpredictable variance through time (Mischke et al., 2013), may have resulted in potential uncertainties. In addition, for sites with limited dating control points (e.g., Kunlun Pass profile, Lake Yanghu), potentially higher uncertainties might be deduced from the constructions of age-depth model.

#### 5.1.2. Low temporal resolution

The criteria for site selection was set as that temporal resolution of fossil pollen record should be higher than 500 years. However, in order to increase the spatial resolution, a few sites with slightly lower temporal resolution were included as well, from regions where limited records were available (e.g., Lake Zabuye and Wumaqu section).

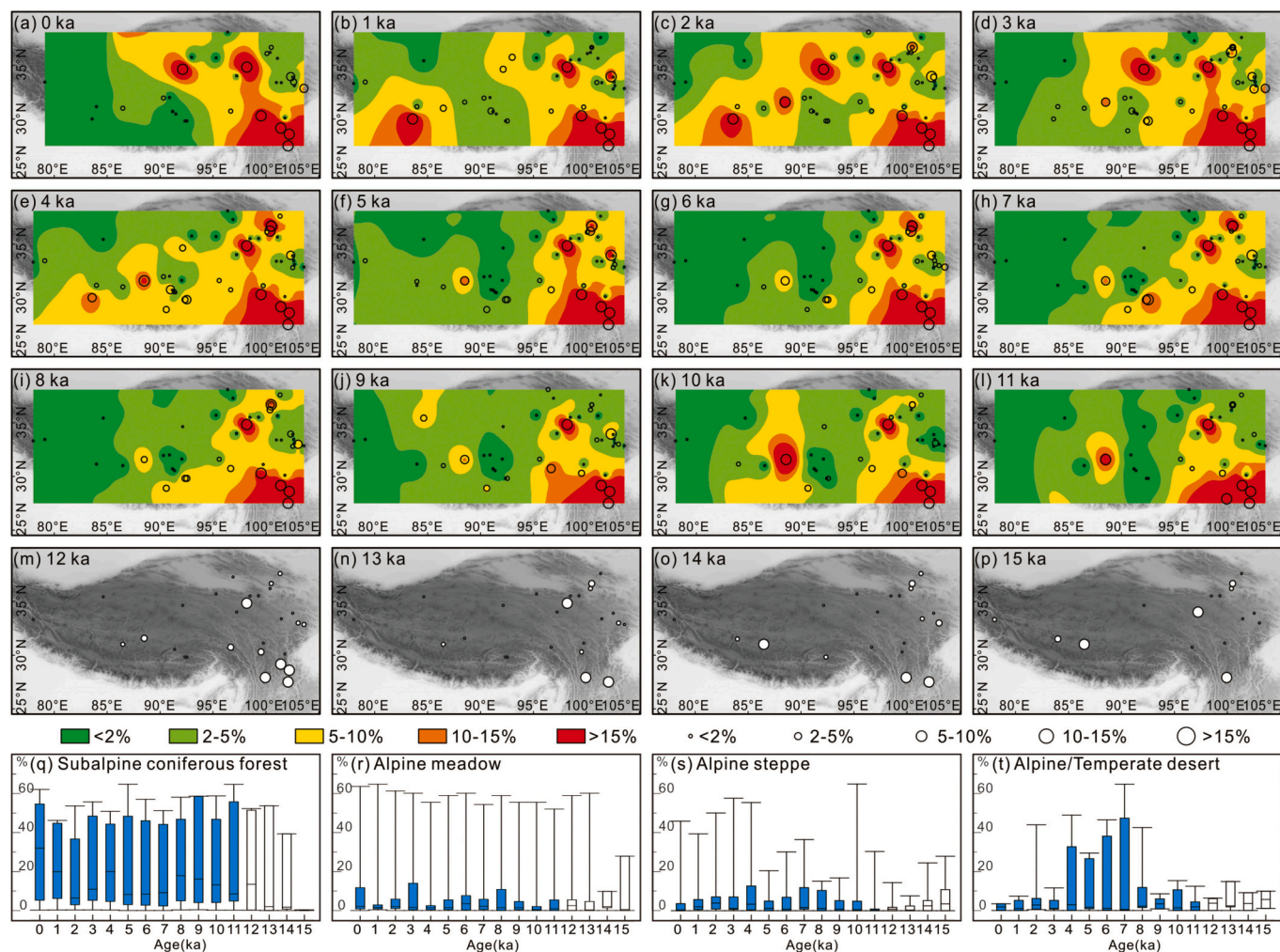


**Fig. 10.** Variation of *Pinus* content in each record (open circles) and spatial interpolations (colored shades) at 1000-year interval for the last 15 kyr (a-p). The boxplots indicate the variation ranges of *Pinus* from four vegetation zones (q-t). The time period between 15 and 12 ka were not interpolated owing to the limited number of records, which were indicated as open boxes as well.

Subsequently, these records with lower temporal resolution may have increased potential uncertainties in spatial analyses and interpolations.

### 5.1.3. Heterogenous spatial distribution

As mentioned above, a few records with slightly lower temporal resolution were included in order to increase the spatial resolution. However, the spatial coverage of the records is still highly heterogenous (Fig. 1). The records were mainly recovered from the southern and eastern parts of the plateau, while only a few records were available from the northern, especially the northwestern QTP. Therefore, the results and inferences of spatial interpolation should be treated with cautions for such regions.

### 5.1.4. Digitization of pollen data

Restricted by the data availability, fossil pollen data from 26 records were acquired by digitization, which may have suffered from potential uncertainties and loss of minor pollen types compared to the raw pollen data. Generally, the principal variations of individual record were captured and represented, providing significant contributions to the fossil pollen dataset and subsequent numerical analyses. Nevertheless, the uncertainties during digitization process may have possibly influenced the results, even for a minor extent.

Due to dating uncertainty, low temporal resolution and the 1000-year wide sampling window, some minor variations may not be fully captured by the interpolated maps either (Giesecke et al., 2017).

Nevertheless, the interpolation of selected pollen types can reflect large-scale patterns in vegetation change and response to climate variations.

## 5.2. Arboreal pollen content as proxy for summer monsoon strength

Traditionally, arboreal pollen content (AP) has been recognized as a useful indicator for evolution of regional vegetation composition (Herzschuh, 2007). Previous studies have noticed that AP detected in the unforested area of QTP were long-distance transported pollen (Lu et al., 2010, 2011). At the meantime, studies also hypothesized that AP were mainly transported by the monsoon current from low altitude areas (Lu et al., 2014). In particular, recent studies on modern pollen samples from the QTP further proved AP as long-distance aeolian transported pollen from southeastern margin of the plateau, which holds the potential to serve as an indicator of monsoon dynamics (Li et al., 2020; Zhang and Li, 2017). The spatial distribution of AP is highly coupled with the path of the ASM and the extent to which it encroached on the QTP (Li et al., 2020). Consequently, the fossil pollen assemblages preserved in the sediments have the potential to track the current direction and intensity of the ASM at that time (Li et al., 2020; Zhang and Li, 2017). The abundant water vapor brought by the ASM nourish the forest vegetation on the southern and eastern parts of QTP, resulting in inextricably linked pollen deposition center and circulation of ASM (Yu et al., 2001).

As the main arboreal taxa preserved in the records, *Betula* and *Abies*/

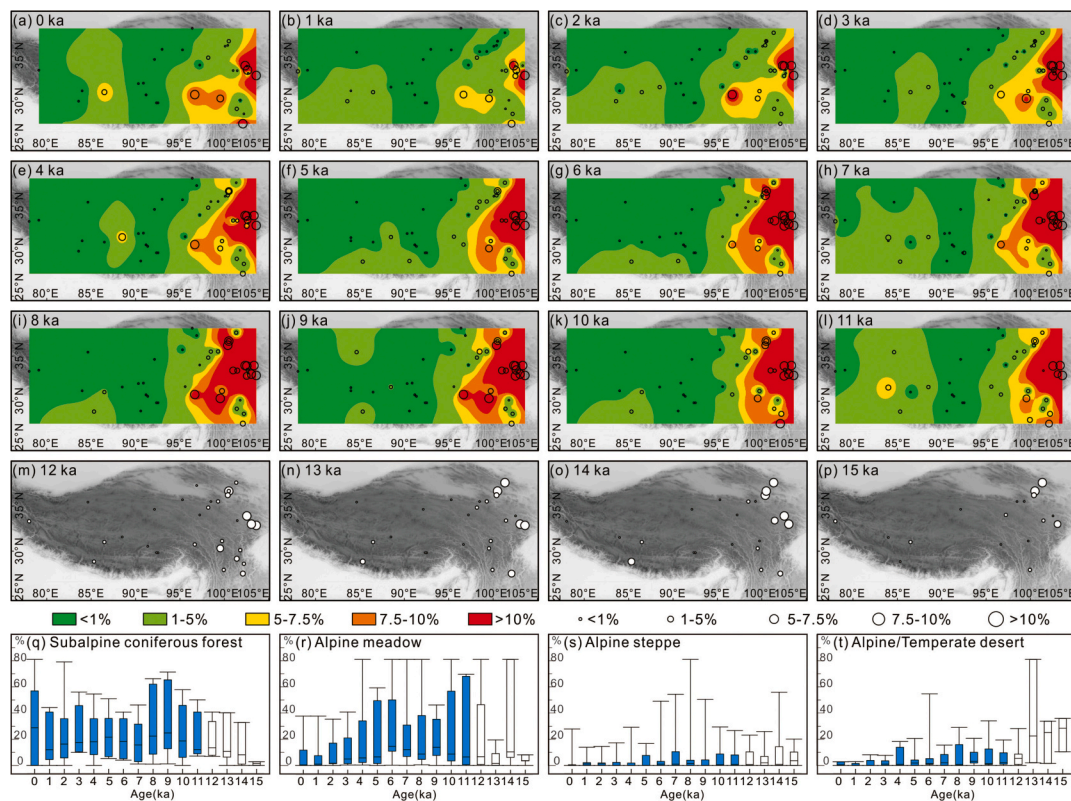


**Fig. 11.** Variation of *Abies/Picea* content in each record (open circles) and spatial interpolations (colored shades) at 1000-year interval for the last 15 kyr (a-p). The boxplots indicate the variation ranges of *Abies/Picea* from four vegetation zones (q-t). The time period between 15 and 12 ka were not interpolated owing the limited number of records, which were indicted as open boxes as well.

*Picea* captured briefly consistent spatial and temporal patterns, showing high contributions in the mountainous area with decreasing gradients towards the northwest across the time slices (Figs. 9, 11), which is consistent with the hypothesis of wind-transported pollen by the summer monsoon (Li et al., 2020; Zhang and Li, 2017). During the early Holocene, the strengthened air flows developed along with the intensification of ASM (Fig. 14; Wang et al., 2005, 2010), which subsequently brought more pollen grains to the central part of plateau, as indicated by the increased pollen proportions in records from alpine meadow, alpine steppe and the deserts (Figs. 9, 11). Then, following the retreat of ASM, the contribution of *Betula* and *Abies/Picea* declined progressively after 7 ka (Figs. 9, 11). On the other hand, *Pinus* showed a much wider spatial distribution and large inter-sites fluctuations (Fig. 10), which is possibly because of its extremely high pollen productivity and dispersal capacity (Li et al., 2018; Schwendemann et al., 2007). Accordingly, *Pinus* pollen grains could be easily transported into the central part of the plateau even without strong monsoon currents, which might not be so sensitive to the variation of monsoon intensity. The spatial distributions of total AP, especially *Pinus* excluded AP (PeAP) revealed by the interpolated maps further represented such wind transported pattern with a northwestward decreasing gradient (Fig. 13). Therefore, the spatial and temporal patterns of arboreal pollen on the plateau could be used as an indicator for the Holocene evolution of summer monsoon, while *Pinus* pollen should be interpreted with more cautions. In addition, the relative proportion of AP is also related to the local pollen content, which may be overestimated especially when high pollen producers invade areas with low pollen producers (Cao et al., 2019). In the era of suitable climate and environment, local vegetation developed and produced a large number of pollen grains, which may reduce the relative percentage of AP. Under harsh conditions, local vegetation was sparse with limited pollen production, that the relative percentage of alien tree pollen might increase.

For the late Glacial (pre-Holocene) period, strong fluctuations were commonly inferred owing to the limited number of available records (Fig. 2d). Generally, the development of regional vegetation before Holocene was constrained by cold and probably arid condition (Herzschuh, 2006; Wang et al., 2005, 2010), revealed by low arboreal pollen content in the subalpine conifer forest area (Fig. 12). Relatively low abundance of AP was also found for the alpine steppe and alpine meadow zones, corresponding to the weak monsoon circulation before Holocene (Herzschuh, 2006; Wang et al., 2005, 2010). For the records from deserts, unexpected high compositions of *Betula*, *Abies/Picea* and PeAP were reported, for instance, Lake Hurleg (Zhao et al., 2007b), which was possible because of extremely low local pollen production (Cheng et al., 2013). In addition, the vegetation coverage was supposed to be sparse during this period according to the low pollen concentrations recovered from Lake Qinghai (Liu et al., 2002), Lake Donggi Cona (Wang et al., 2014), Lake Kuhai (Wischnewski et al., 2011), Kunlun Pass (Liu et al., 1997), Tangra Yumco (Ma et al., 2019a, 2019b), and Lake Shudu (Cook et al., 2011), as well as low pollen accumulation rate from Lake Naleng (Kramer et al., 2010b) and low pollen influx from Tso Kar (Demske et al., 2009). The vegetation signals revealed by the fossil pollen records expressed broad consistence with climate variations retrieved from various archives, for instance, stalagmite records (Dongge Cave, Dykoski et al., 2005; Timta Cave, Sinha et al., 2005), ice core (GISP2, Grootes et al., 1993), marine sediments (Overpeck et al., 1996; Sirocko et al., 1993) and synthesized moisture indices (Herzschuh, 2006; Wang et al., 2010, 2017).

During early to mid-Holocene period (approximately 12–7 ka), the overall climate condition on the QTP was warm and humid, which is suitable for local vegetation development, as reported from various record on the plateau (Chen et al., 2020). At the meantime, the individual arboreal taxon, together with total AP content revealed high proportions in the pollen assemblages, especially the period between 9 and 7 ka

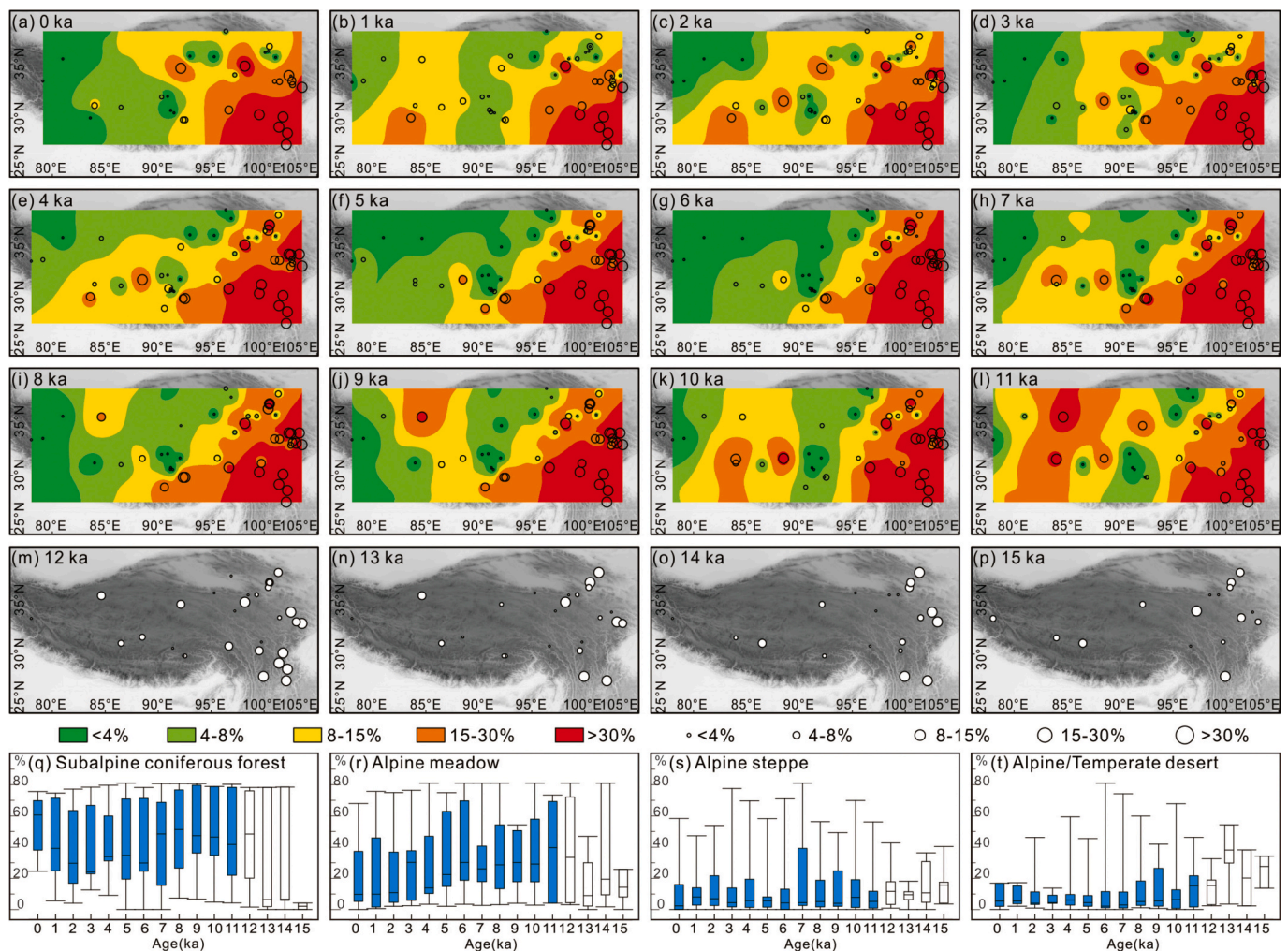


**Fig. 12.** Variation of Arboreal Pollen content in each record (open circles) and spatial interpolations (colored shades) at 1000-year interval for the last 15 kyr (a-p). The boxplots indicate the variation ranges of Arboreal Pollen from four vegetation zones (q-t). The time period between 15 and 12 ka were not interpolated owing to the limited number of records, which were indicated as open boxes as well.

(Figs. 9–13), further indicating that more tree pollen grains were blown into the plateau by strengthened summer monsoon. Accordingly, high values were detected from both the proportion of arboreal pollen in each record and the area covered by high arboreal pollen during this period. The stable oxygen isotope records of stalagmites from Dongge Cave indicated that the maximal monsoon was formed during the early Holocene (Dykoski et al., 2005; Wang et al., 2005), which is broadly consistent with the inferences of synthesized fossil pollen record (Fig. 14).

During the mid-Holocene, the ASM retreated gradually following the decline of Northern Hemisphere summer solar insolation (Wang et al., 2010). Recent investigation from western Yunnan Plateau indicated that regional vegetation changed abruptly at about 5.2 ka together with the decline of summer monsoon (Wang et al., 2020), with consistent conclusions as the synthesis of published paleoclimatic records (Morrill et al., 2003) and various sedimentary records from the QTP (e.g., Zhang et al., 2016). During this period, the AP pollen content decreased significantly across the plateau (Fig. 12), representing the retreating process of summer monsoon.

For the late Holocene (4–0 ka), the AP content especially *Betula* in the subalpine forest zone decreased significantly, indicating a more open landscape corresponding to the retreat of ASM (Kramer et al., 2010a). Generally, decreasing trends in AP were noticed in the alpine steppe and alpine meadow zones as well (Figs. 12, 13), owing to the reduced pollen production in the forest area in combination with the weakened

monsoon circulation (Wang et al., 2005). A slight increase appeared in the records from the desert area (Figs. 12, 13), as a result of reduced local pollen production, which is briefly consistent with the pre-Holocene conditions. In addition, *Pinus* pollen content showed strong fluctuations during the mid to late Holocene period, further approving that *Pinus* pollen could be more easily transported to the interior of the plateau.

The synthesis of arboreal pollen content from QTP records confirms its application in tracking Holocene variation of summer monsoon intensity, which is broadly consistent with the hypothesis proposed by Li et al. (2020). Meanwhile, as a commonly reported pollen type, *Pinus* pollen should be interpreted with care both in terms of regional vegetation change and potential indication for summer monsoon circulation dynamics. According to the spatial and temporal patterns of AP, the evolution ASM since late Glacial could be briefly reconstructed. The summer monsoon strengthened after the transition from late Glacial to Holocene, maintained at a high level during early to mid-Holocene and declined roughly after 6 ka.

### 5.3. Response of non-arboreal pollen composition on the QTP to monsoon evolution

The non-arboreal pollen species, including major shrub and herbaceous pollen, are considered to be mainly of local origin, which represents the development of regional vegetation compositions following

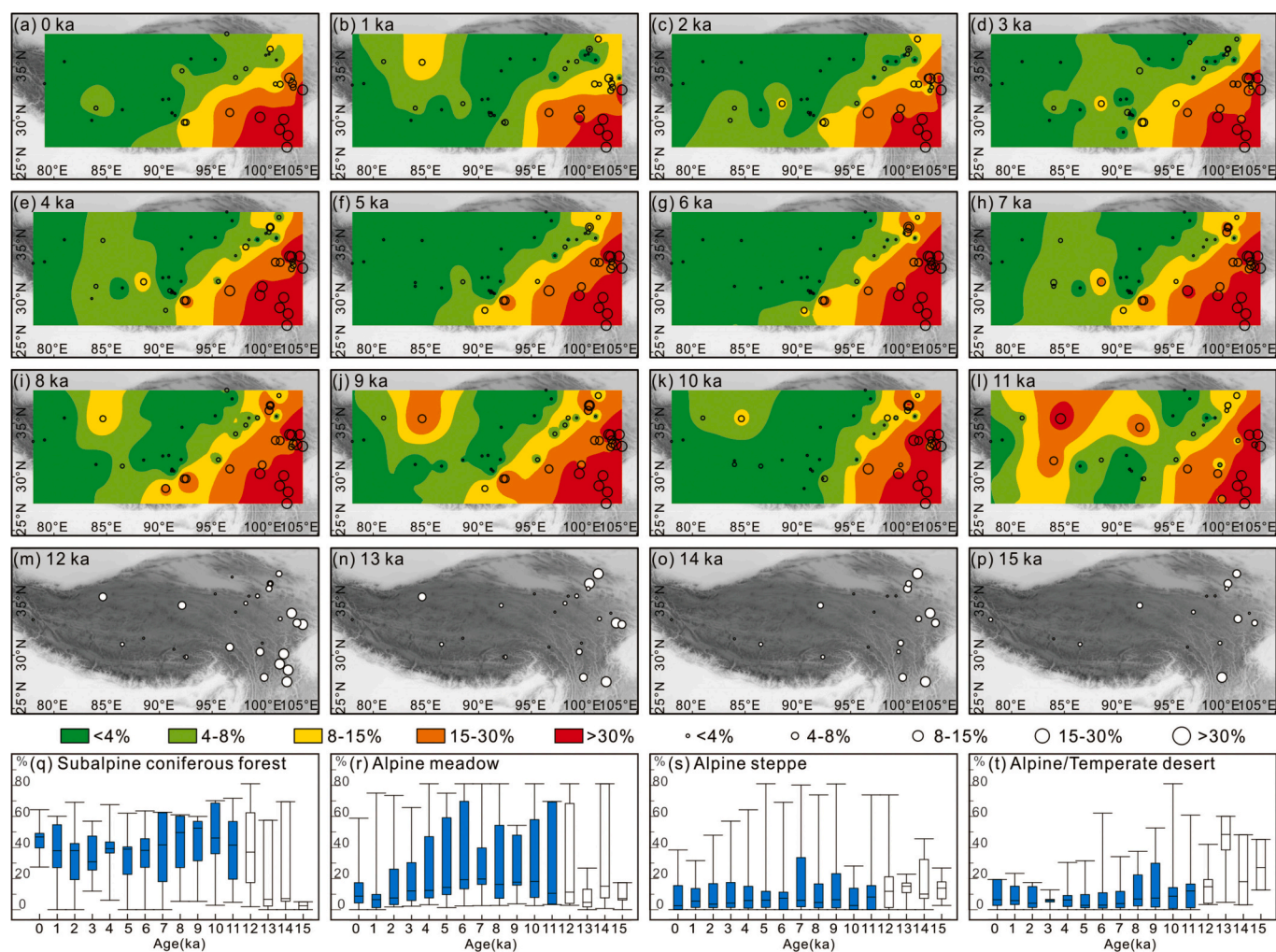


**Fig. 13.** Variation of *Pinus*-excluded Arboreal Pollen content in each record (open circles) and spatial interpolations (colored shades) at 1000-year interval for the last 15 kyr (a-p). The boxplots indicate the variation ranges of *Pinus*-excluded Arboreal Pollen from four vegetation zones (q-t). The time period between 15 and 12 ka were not interpolated owing the limited number of records, which were indicated as open boxes as well.

climate variations (Cour et al., 1999; Li, 2018; Li et al., 2020; Shen et al., 2006).

Pollen grains from *Artemisia* and *Chenopodiaceae* are commonly preserved in the Holocene records on the QTP (Ren and Beug, 2002), which shows dominant compositions in the alpine steppe and desert biomes (Figs. 3, 4). Consequently, the *Artemisia*/*Chenopodiaceae* ratio (A/C) has been used to distinguish regional vegetation composition and moisture conditions based on investigations of modern surface pollen composition from QTP (e.g., Cour et al., 1999; Herzsuh, 2007; Ma et al., 2017; Shang et al., 2009; Wei et al., 2011) and arid/semi-arid areas in northwestern China (e.g., Qin et al., 2015; Wei and Zhao, 2016; Zhao and Li, 2013; Zhao et al., 2012a). Besides the concerns about potential biases from local vegetation composition or pollen dispersal process (Zhang et al., 2018; Zhao et al., 2021), the A/C ratio has been widely approved to correlate positively with regional moisture/precipitation conditions (Li et al., 2010; Zhao et al., 2012b). Poaceae pollen was identified over the whole plateau owing to the wide distribution of Poaceae plants (e.g., *Stipa purpurea*) and its strong adaptability (Fig. 7). Besides the indication of vegetation and climate changes, Poaceae pollen was also used to reflect human activities since it contains various agricultural species (Bush, 2002; Hicks and Birks, 1996; Zhou et al., 2008). As the dominant pollen type of alpine meadow (Zhou, 2001), higher proportions of Cyperaceae in the records generally indicate expansions of meadow component (i.e., *Kobresia* species), referring to possible increase of regional moisture conditions (Sun et al., 2017; Yan et al.,

1999). On the other hand, relatively dry conditions could be derived from the high compositions of *Ephedra*, which is widely distributed in the desert landscape (Herzsuh et al., 2004).

During the late Glacial period, high proportions of *Ephedra* and *Chenopodiaceae* appeared in the records from alpine steppe and alpine meadow zones, with noticeable values in the subalpine forest area (Fig. 8), indicating the prevailed cold/dry conditions (Herzsuh, 2006; Wang et al., 2005). At the meantime, extremely low values from the deserts are probably resulted from sparse local vegetation coverage and low pollen production under the harsh condition, as indicated by the extremely low values of pollen concentration or pollen influx (Demske et al., 2009; Liu et al., 2002). Subsequently, long-way transported arboreal pollen showed high contributions during this period as we discussed above (Figs. 12, 13). In addition, high proportions of Cyperaceae were reported from the present subalpine forest area reaching up to 60% (Fig. 6), which represented the development of alpine meadow during the late Glacial period according to the investigations of modern pollen assemblages on the QTP (Li et al., 2020; Yu et al., 2001). In other words, the high Cyperaceae content indicated possible southward expansions of alpine meadow under relatively cold/dry late Glacial condition (Kramer et al., 2010b), which is broadly consistent with the simulated forest retreat in BIOME4 (Ni et al., 2010). Such replacement of subalpine forest by alpine meadow further confirmed the overall cold/dry condition during the last Glacial, which has been widely proposed in the paleoclimate records (e.g., Dykoski et al., 2005; Grootes et al., 1993;

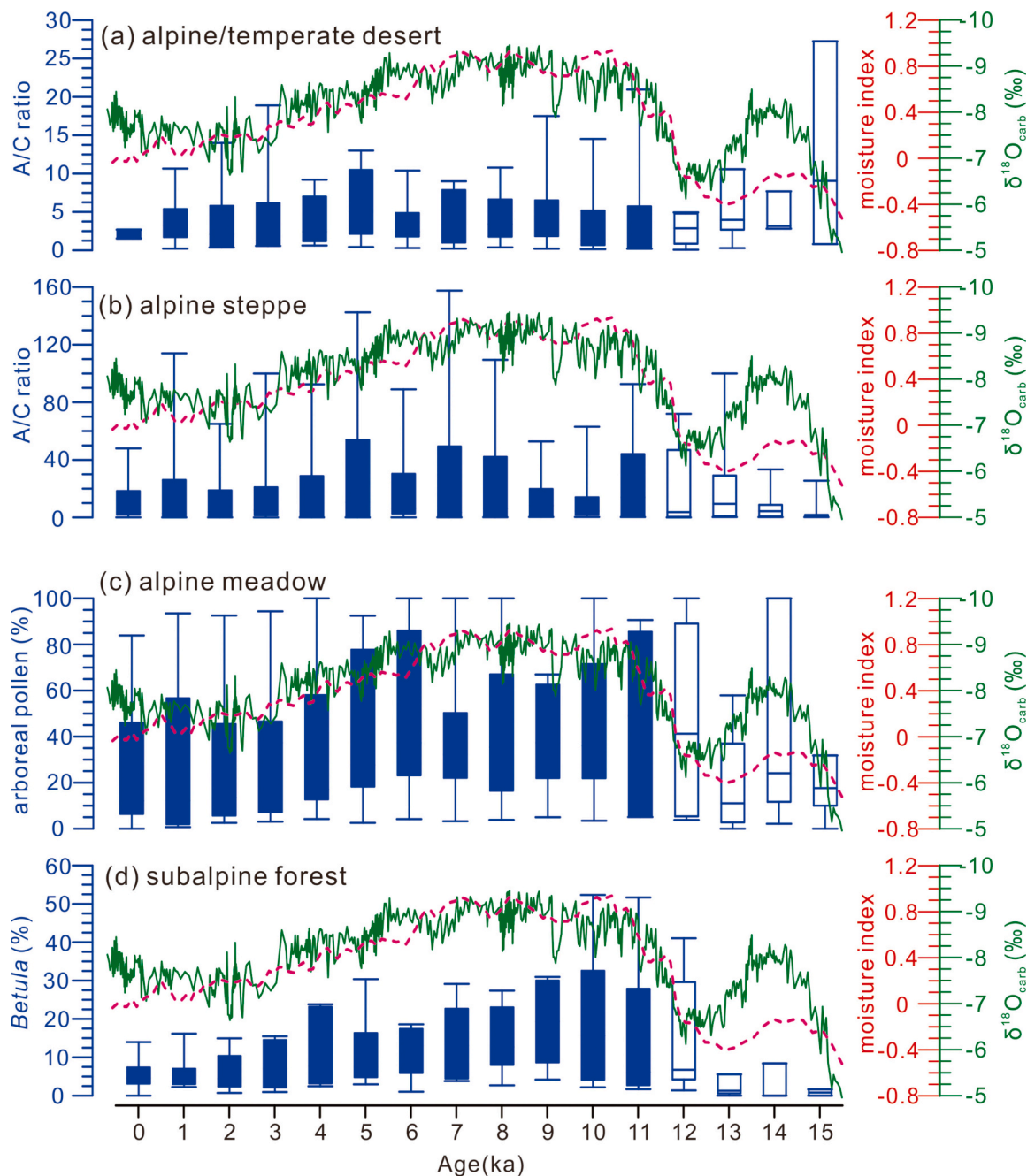


**Fig. 14.** Comparison of *Artemisia*/Chenopodiaceae ratios (A/C) from alpine steppe (a) and alpine/temperate desert (b) zones, (c) arboreal pollen content in alpine meadow zone, and (d) *Betula* content in subalpine forest zone, with stable oxygen isotope records from Dongge Cave (green lines, Wang et al., 2005) and mean moisture indices from monsoonal central Asia (red dashed lines, Wang et al., 2010). (For interpretation of the references to colour in this figure legend, the reader is referred to the web version of this article.)

Overpeck et al., 1996; Sinha et al., 2005; Sirocko et al., 1993).

In the northwestern part of the plateau, *Artemisia* content increased gradually in the early Holocene between 11 and 7 ka (Fig. 3), along with relatively low values of Chenopodiaceae (Fig. 4) as well as increased A/C ratios (Fig. 5), indicating that the climate became humid under the intensified summer monsoon circulation (Fig. 14; Wang et al., 2005, 2010). Identical patterns could be inferred from the central plateau of alpine steppe and alpine meadow zones that Chenopodiaceae content decreased significantly, together with increasing A/C ratios (Figs. 4, 5), corresponding to increased available moisture. Furthermore, such wetting trend was also confirmed by the expansion of Cyperaceae to desert and steppe regions (Fig. 6).

For the mid to late Holocene period after 7 ka, progressive declines of

*Artemisia* and Cyperaceae could be noticed for the alpine steppe and alpine meadow zones (Figs. 3, 6), indicating decrease of regional moisture condition following the retreat of summer monsoon (Chen et al., 2020; Wang et al., 2005). Consistently, the proportions of Chenopodiaceae expressed increasing trends, particularly for the desert areas, which further proves the process towards an arid environment. Meanwhile, the forest landscape in the southeastern margin of QTP became more open during this stage as indicated by the expansion of Cyperaceae (Figs. 6, 12).

In addition, the content of Poaceae expressed a generally stable pattern, with a gradual increasing trend after 7 ka as well as spatial expansions in the northeastern QTP (Fig. 7), which may be closely related to human activities. Previous synthesis of fossil pollen records on

the QTP revealed close correlation between vegetation change and human activities (Hou et al., 2017a, 2017b). The microblade remains have been widely discovered from the northeastern QTP, which was dated back to even the early Holocene (Madsen et al., 2006; Tang, 1999), and reached its maximum between 8.8 and 6 ka owing to expansion of humans to the northeastern QTP under the relatively warm and wet condition (Hou et al., 2017a, 2017b). As a result, the increase of Poaceae content may have been caused by intensified human impacts during this period.

The development of local vegetation composition of the QTP could be represented by variations of major herbaceous pollen proportions, i. e., *Artemisia*, Chenopodiaceae and Cyperaceae. In the meantime, the variation of Poaceae pollen, especially the increase during the mid to late Holocene period, showed a close correlation with possible regional human activities.

## 6. Conclusions

Based on the spatial interpolation of major pollen types from 57 records covering the past 15,000 years, temporal and spatial variations of alpine vegetation on the Qinghai-Tibetan Plateau since the late Glacial were investigated. The pollen mapping results at 1000-year interval successfully represented regional vegetation evolution and underlying climate processes. The overall condition during the late Glacial was generally cold and dry, as indicated by low arboreal pollen content from the subalpine forest zone (more open landscape) and high proportions in the unforested region (as exotic pollen due to limited local pollen production). Based on the spreading pattern of arboreal pollen (e. g., *Betula*, *Abies/Picea*) on the plateau, the Holocene evolution history of ASM was briefly established, showing strengthened conditions during the early to mid-Holocene, which declined after about 7 ka. The local vegetation developments revealed by shrub and herbaceous species (i.e., *Artemisia*, Chenopodiaceae, Poaceae, Cyperaceae and *Ephedra*), captured the overall climate variations as well. Particularly, expansion of Poaceae in northeastern plateau after 7 ka indicated possible influences of human activities. The synthesis provides necessary references for understanding long-term vegetation evolution and reconstructing past climate/environment changes on the QTP, which is of great significance for the investigation of the monsoon dynamics and the responding process of alpine ecosystem to the monsoon variation.

## Declaration of Competing Interest

The authors declare that they have no known competing financial interests or personal relationships that could have appeared to influence the work reported in this paper.

## Acknowledgements

We thank Dr. Xiaozhong Huang, Dr. Yun Zhang, Dr. Yunfa Miao, Dr. Bo Cheng, Dr. Enlou Zhang, Dr. Zhenyu Ni, and other palynologists for providing the original fossil pollen data. The study was financially supported by the National Natural Science Foundation of China (No. 41877282, 41861134030) and Capital Normal University. We are grateful to the editors, Prof. Dr. Thomas Algeo, Prof. Dr. Howard Falcon-Lang, and two anonymous referees for their constructive suggestions that improved our manuscript.

## Appendix A. Supplementary data

Supplementary data to this article can be found online at <https://doi.org/10.1016/j.palaeo.2021.110412>.

## References

- An, Z., Kutzbach, J.E., Prell, W.L., Porter, S.C., 2001. Evolution of Asian monsoon and phased uplift of the Himalaya-Tibetan Plateau since Late Miocene times. *Nature* 411, 62–66.
- Bernabo, J.C., Webb III, T., 1977. Changing patterns in the Holocene pollen record of northeastern North America: a mapped summary. *Quat. Res.* 8, 64–96.
- Blaauw, M., Christen, J.A., 2011. Flexible paleoclimate age-depth models using an autoregressive gamma process. *Bayesian Anal.* 6, 457–474.
- Brewer, S., Giesecke, T., Davis, B.A.S., Finsinger, W., Wolters, S., Binney, H., Beaulieu, J. L.D., Fyfe, R., Gil-Romera, G., Kühl, N., Kunes, P., Leydet, M., Bradshaw, R.H., 2017. Late-glacial and Holocene European pollen data. *J. Maps.* 13, 921–928.
- Bush, M.B., 2002. On the interpretation of fossil Poaceae pollen in the lowland humid neotropics. *Paleogeogr. Paleoclimatol. Paleocol.* 177, 5–17.
- Campo, E.V., Cour, P., Hang, S., 1996. Holocene environmental changes in Bangong Co Basin (Western Tibet). part 2: the pollen record. *Paleogeogr. Paleoclimatol. Paleocol.* 120, 49–63.
- Campo, E.V., Gasse, F., 1993. Pollen and diatom inferred climatic and hydrological changes in Sumxi Co Basin (Western Tibet) since 13,000 yr B.P. *Quat. Res.* 39, 300–313.
- Cao, X., Herzsich, U., Ni, J., Zhao, Y., Böhmer, T., 2014. Spatial and temporal distributions of major tree taxa in eastern continental Asia during the last 22,000 years. *Holocene.* 25, 79–91.
- Cao, X., Ni, J., Herzsich, U., Wang, Y., Zhao, Y., 2013. A late quaternary pollen dataset from eastern continental Asia for vegetation and climate reconstructions: set up and evaluation. *Rev. Palaeobot. Palynol.* 194, 21–37.
- Cao, X., Tian, F., Li, F., Gaillard, M.J., Herzsich, U., 2019. Pollen-based quantitative land-cover reconstruction for northern Asia covering the last 40 ka cal BP. *Clim. Past* 15, 1503–1536.
- Chang, D., 1983. The Tibetan Plateau in relation to the vegetation of China. *Ann. Mo. Bot. Gard.* 70, 564–570.
- Chen, F., Chen, J., Huang, W., Chen, S., Huang, X., Jin, L., Jia, J., Zhang, X., An, C., Zhang, J., Zhao, Y., Yu, Z., Zhang, R., Liu, J., Zhou, A., Feng, S., 2019. Westerlies Asia and monsoonal Asia: Spatiotemporal differences in climate change and possible mechanisms on decadal to sub-orbital timescales. *Earth-Sci. Rev.* 192, 337–354.
- Chen, F., Zhang, J., Liu, J., Cao, X., Hou, J., Zhu, L., Xu, X., Liu, X., Wang, M., Wu, D., Huang, L., Zeng, T., Zhang, S., Huang, W., Zhang, X., Yang, K., 2020. Climate change, vegetation history, and landscape responses on the Tibetan Plateau during the Holocene: A comprehensive review. *Quat. Sci. Rev.* 243, 106444.
- Cheng, B., Chen, F., Zhang, J., 2013. Palaeovegetational and palaeoenvironmental changes since the last deglacial in Gonghe Basin, northeast Tibetan Plateau. *J. Geogr. Sci.* 23, 136–146.
- Cheng, J., Zhang, X., Tian, M., Tang, D., Yu, W., Yu, J., Qiao, G., Zan, L., 2004. Climate of the Holocene megathermal in the source area of the Yellow River, Northeast Tibet. *Geol. Rev.* 3, 330–337 (in Chinese with English abstract).
- Cheng, M., Zong, Y., Zheng, Z., Huang, K., Aitchison, J.C., 2014. A stable mid-late Holocene monsoon climate of the central Tibetan Plateau indicated by a pollen record. *Quat. Int.* 333, 40–48.
- Cook, C., Jones, R., Langdon, P., Leng, M., Zhang, E., 2011. New insights on late quaternary Asian palaeomonsoon variability and the timing of the last Glacial Maximum in southwestern China. *Quat. Sci. Rev.* 30, 808–820.
- Cour, P., Zheng, Z., Duzer, D., Calleja, M., Yao, Z., 1999. Vegetational and climatic significance of modern pollen rain in northwestern Tibet. *Rev. Palaeobot. Palynol.* 104, 183–204.
- Liu, G., Cui, Z., Wu, Y., Xu, Q., 1997. Record of environmental change in Reshui profile at Kunlunshan Pass since 18 ka BP. *Int. J. Geomech.* 4, 41–47 (in Chinese with English abstract).
- Demske, D., Tarasov, P.E., Wuenemann, B., Riedel, F., 2009. Late Glacial and Holocene vegetation, Indian monsoon and westerly circulation in the Trans-Himalaya recorded in the lacustrine pollen sequence from Tso Kar, Ladakh, NW India. *Paleogeogr. Paleoclimatol. Paleocol.* 279, 172–185.
- Du, N., Kong, Z., Shan, F., 1989. A preliminary investigation on the vegetational and climatic changes since 11000 years in Qinghai Lake: an analysis based on palynology in core QH85-14C. *Acta Bot. Sin.* 31, 803–814 (in Chinese with English abstract).
- Dykoski, C.A., Edwards, R.L., Cheng, H., Yuan, D., Cai, Y., Zhang, M., Lin, Y., Qing, J., An, Z., Revenaugh, J., 2005. A high-resolution, absolute-dated Holocene and Deglacial Asian Monsoon record from Dongge cave, China. *Earth Planet. Sci. Lett.* 233, 71–86.
- Gajewski, K., 2008. The Global Pollen Database in biogeographical and palaeoclimatic studies. *Prog. Phys. Geogr.* 32, 379–402.
- Gasse, F., Arnold, M., Fontes, J.C., Fort, M., Gibert, E., Huc, A., Li, B., Li, F., Liu, Q., Mélières, F., Campo, E.V., Wang, F., Zhang, Q., 1991. A 13,000-year climate record from western Tibet. *Nature.* 353, 742–745.
- Giesecke, T., Brewer, S., 2018. Notes on the postglacial spread of abundant European tree taxa. *Veg. Hist. Archaeobot.* 27, 337–349.
- Giesecke, T., Brewer, S., Finsinger, W., Leydet, M., Bradshaw, R.H.W., 2017. Patterns and dynamics of European vegetation change over the last 15,000 years. *J. Biogeogr.* 44, 1441–1456.
- Giesecke, T., Davis, B., Brewer, S., Finsinger, W., Wolters, S., Blaauw, M., de Beaulieu, J., Binney, H., Fyfe, R.M., Gaillard, M.J., Gil-Romera, G., van der Knaap, W.O., Kunes, P., Kuehl, N., van Leeuwen, J.F.N., Leydet, M., Lotter, A.F., Ortu, E., Semmler, M., Bradshaw, R.H.W., 2014. Towards mapping the late Quaternary vegetation change of Europe. *Veg. Hist. Archaeobot.* 23, 75–86.
- Groote, P.M., Stuiver, M., White, J.W.C., Johnsen, S., Jouzel, J., 1993. Comparison of oxygen isotope records from the GISP2 and GRIP Greenland cores. *Nature.* 366, 552–554.



- Herrmann, M., Lu, X., Berking, J., Schuett, B., Yao, T., Mosbrugger, V., 2010. Reconstructing Holocene vegetation and climate history of Nam Co area (Tibet), using pollen and other palynomorphs. *Quat. Int.* 218, 45–57.
- Herzschuh, U., 2006. Palaeo-moisture evolution in monsoonal Central Asia during the last 50,000 years. *Quat. Sci. Rev.* 25, 163–178.
- Herzschuh, U., 2007. Reliability of pollen ratios for environmental reconstructions on the Tibetan Plateau. *J. Biogeogr.* 34, 1265–1273.
- Herzschuh, U., Borkowski, J., Schewe, J., Mischke, S., Tian, F., 2014. Moisture-advection feedback supports strong early-to-mid Holocene monsoon climate on the eastern Tibetan Plateau as inferred from a pollen-based reconstruction. *Paleogeogr. Paleoclimatol. Paleoecol.* 402, 44–54.
- Herzschuh, U., Cao, X., Laepple, T., Dallmeyer, A., Telford, R.J., Ni, J., Chen, F.H., Kong, Z.C., Liu, G.X., Liu, K.B., Liu, X.Q., Stebich, M., Tang, L.Y., Tian, F., Wang, Y. B., Wischnewski, J., Xu, Q.H., Yan, S., Yang, Z.J., Yu, G., Zhang, Y., Zhao, Y., Zheng, Z., 2019. Position and orientation of the westerly jet determined Holocene rainfall patterns in China. *Nat. Commun.* 10, 2376.
- Herzschuh, U., Kramer, A., Mischke, S., Zhang, C., 2009. Quantitative climate and vegetation trends since the late glacial on the northeastern Tibetan Plateau deduced from Koucha Lake pollen spectra. *Quat. Res.* 71, 162–171.
- Herzschuh, U., Tarasov, P., Winnemann, B., Hartmann, K., 2004. Holocene vegetation and climate of the Alashan Plateau, NW China, reconstructed from pollen data. *Paleogeogr. Paleoclimatol. Paleoecol.* 211, 1–17.
- Herzschuh, U., Winter, K., Wünnemann, B., Li, S., 2006. A general cooling trend on the central Tibetan Plateau throughout the Holocene recorded by the Lake Zigetang pollen spectra. *Quat. Int.* 154–155, 113–121.
- Herzschuh, U., Zhang, C., Mischke, S., Herzschuh, R., Mohammadi, F., Ingram, B., Kürschner, H., Riedel, F., 2005. A late quaternary lake record from the Qilian Mountains (NE China): evolution of the primary production and the water depth reconstructed from macrofossil, pollen, biomarker, and isotope data. *Glob. Planet. Chang.* 46, 361–379.
- Hicks, S., Birks, H.J.B., 1996. Numerical analysis of modern and fossil pollen spectra as a tool for elucidating the nature of fine-scale human activities in boreal areas. *Veg. Hist. Archaeobot.* 5, 257–272.
- Hou, X., 2001. *Vegetation Atlas of China*. Science Press, Beijing (in Chinese).
- Hou, J., Dandrea, W.J., Liu, Z., 2012. The influence of  $^{14}\text{C}$  reservoir age on interpretation of paleolimnological records from the Tibetan Plateau. *Quat. Sci. Rev.* 48, 67–79.
- Hou, J., Dandrea, W.J., Wang, M., He, Y., Liang, J., 2017a. Influence of the Indian monsoon and the subtropical jet on climate change on the Tibetan Plateau since the late Pleistocene. *Quat. Sci. Rev.* 163, 84–94.
- Hou, G., Yang, P., Cao, G., Chongyi, E., Wang, Q., 2017b. Vegetation evolution and human expansion on the Qinghai-Tibet Plateau since the Last Deglaciation. *Quat. Int.* 430, 82–93.
- Huang, F., 2000. Vegetation and climate between 13 ka to 5ka B.P. in Peiku Co, Tibet. *Acta Palaeontol. Sin.* 3, 441–448 (in Chinese with English abstract).
- Huang, X., Liu, S., Dong, G., Qiang, M., Bai, Z., Zhao, Y., Chen, F., 2017. Early human impacts on vegetation on the northeastern Qinghai-Tibetan Plateau during the middle to late Holocene. *Prog. Phys. Geogr.* 41, 286–301.
- Huntley, B., 2010. European vegetation history: Palaeovegetation maps from pollen data –13 000 yr BP to present. *J. Quat. Sci.* 5, 103–122.
- Huntley, B., Birks, H.J.B., 1983. *An Atlas of Past and Present Pollen Maps for Europe: 0–13000 Years Ago*. Cambridge University Press, Cambridge.
- Immerzeel, W.W., Lutz, A.F., Andrade, M., Bahl, A., Biemans, H., Bolch, T., Hyde, S., Brumby, S., Davies, B.J., Elmore, A.C., Emmer, A., Feng, M., Fernandez, A., Haritashya, U., Kargel, J.S., Koppes, M., Kraaijenbrink, P.D.A., Kulkarni, A.V., Mayewski, P.A., Nepal, S., Pacheco, P., Painter, T.H., Pellicciotti, F., Rajaram, H., Rupper, S., Sinisalo, A., Shrestha, A.B., Viviroli, D., Wada, Y., Xiao, C., Yao, T., Baillie, J.E.M., 2020. Importance and vulnerability of the world's water towers. *Nature*. 577, 364–369.
- Jarvis, D.L., 1993. Pollen evidence of changing Holocene monsoon climate in Sichuan province, China. *Quat. Res.* 39, 325–337.
- Kramer, A., Herzschuh, U., Mischke, S., Zhang, C., 2010a. Holocene treeline shifts and monsoon variability in the Hengduan Mountains (southeastern Tibetan Plateau) implications from palynological investigations. *Paleogeogr. Paleoclimatol. Paleoecol.* 286, 23–41.
- Kramer, A., Herzschuh, U., Mischke, S., Zhang, C., 2010b. Late glacial vegetation and climate oscillations on the southeastern Tibetan Plateau inferred from the Lake Naleng pollen profile. *Quat. Res.* 73, 324–335.
- Li, Q., 2018. Spatial variability and long-term change in pollen diversity in Nam Co catchment (central Tibetan Plateau): implications for alpine vegetation restoration from a paleoecological perspective. *Sci. China Earth Sci.* 61, 270–284.
- Li, F., Gaillard, M.J., Cao, X., Herzschuh, U., Sugita, S., Tarasov, P.E., Wagnere, M., Xu, Q., Ni, J., Wang, W., Zhao, Y., An, C., Beusen, A.H.W., Chen, F., Feng, Z., Goldewijk, C.G.M.K., Huang, X., Li, Y., Liu, H., Sun, A., Yao, Y., Zheng, Z., Jia, X., 2019. Towards quantification of Holocene anthropogenic land-cover change in temperate China: a review in the light of pollen-based REVEALS reconstructions of regional plant cover. *Earth-Sci. Rev.* 203, 103119.
- Li, F., Gaillard, M.J., Xu, Q., Bunting, M.J., Li, Y., Li, J., Mu, H., Lu, J., Zhang, P., Zhang, S., Cui, Q., Zhang, Y., Shen, W., 2018. A review of relative pollen productivity estimates from temperate China for pollen-based quantitative reconstruction of past plant cover. *Front. Plant Sci.* 9, 1214.
- Li, X., Liu, J., 1988. Holocene vegetational and environmental changes at Mt. Luoji, Sichuan. *Acta Geograph. Sin.* 1, 44–51 (in Chinese with English abstract).
- Li, F., Sun, J., Zhao, Y., Guo, X., Zhao, W., Zhang, K., 2010. Ecological significance of common pollen ratios: a review. *Front. Earth Sci. China.* 4, 253–258.
- Li, J., Xie, G., Yang, J., Ferguson, D.K., Liu, X., Liu, H., Wang, Y., 2020. Asian Summer Monsoon changes the pollen flow on the Tibetan Plateau. *Earth-Sci. Rev.* 202, 103114.
- Liu, S., Huang, X., Qiang, M., Lin, X., Bai, Z., Peng, W., 2016. Vegetation and climate change during the mid-late Holocene reflected by the pollen record from Lake Genggahai northeastern Tibetan Plateau. *Quat. Sci.* 36, 247–256 (in Chinese with English abstract).
- Liu, G., Shen, Y., Wang, S., 1995. The Vegetation and Climate of Holocene Megathermal in Zoige, Northwestern Sichuan, China. *J. Glaciol. Geocryol.* 03, 247–249 (in Chinese with English abstract).
- Liu, X., Shen, J., Wang, S., Yang, X., Tong, G., Zhang, E., 2002. A 16000-year pollen record of Qinghai Lake and its paleoclimate and paleoenvironment. *Chin. Sci. Bull.* 47, 1931–1936.
- Liu, K., Yao, Z., Thompson, L.G., 1998. A pollen record of Holocene climatic changes from the Dunde ice cap, Qinghai-Tibetan Plateau. *Geology.* 26, 135–138.
- Lu, X., Herrmann, M., Mosbrugger, V., Yao, T., Zhu, L., 2010. Airborne pollen in the Nam Co Basin and its implication for palaeoenvironmental reconstruction. *Rev. Palaeobot. Palynol.* 163, 104–112.
- Lu, H., Wang, S., Shen, C., Yang, X., Tong, G., Liu, K., 2014. Spatial pattern of modern *Abies* and *Picea* pollen in the Qinghai-Xizang Plateau. *Quat. Int.* 24, 39–49.
- Lu, H., Wu, N., Liu, K., Zhu, L., Yang, X., Yao, T., Wang, L., Li, Q., Liu, X., Shen, C., 2011. Modern pollen distributions in Qinghai-Tibetan Plateau and the development of transfer functions for reconstructing Holocene environmental changes. *Quat. Sci. Rev.* 30, 947–966.
- Ma, Q., Zhu, L., Lu, X., Guo, Y., Ju, J., Wang, J., Wang, Y., Tang, L., 2014. Pollen-inferred Holocene vegetation and climate histories in Taro Co, southwestern Tibetan Plateau. *Chin. Sci. Bull.* 59, 4101–4114.
- Ma, Q., Zhu, L., Lu, X., Wang, J., Ju, J., Kasper, T., Daut, G., Haberzettl, T., 2019b. Late Glacial and Holocene vegetation and climate variations at Lake Tangra Yumco, central Tibetan Plateau. *Glob. Planet. Chang.* 174, 16–25.
- Ma, Q., Zhu, L., Wang, J., Ju, J., Lu, X., Wang, Y., Guo, Y., Yang, R., Kasper, T., Haberzettl, T., Tang, L., 2017. *Artemisia*/Chenopodiaceae ratio from surface lake sediments on the central and western Tibetan Plateau and its application. *Paleogeogr. Paleoclimatol. Paleoecol.* 479, 138–145.
- Ma, Q., Zhu, L., Wang, J., Ju, J., Wang, Y., Lu, X., Kasper, T., Haberzettl, T., 2019a. Late Holocene vegetation responses to climate change and human impact on the central Tibetan Plateau. *Sci. Total Environ.* 708, 135370.
- Madsen, D.B., Ma, H., Brantingham, P.J., Gao, X., Rhode, D., Zhang, H., Olsen, J.W., 2006. The Late Upper Paleolithic occupation of the northern Tibetan Plateau margin. *J. Archaeol. Sci.* 33, 1433–1444.
- Miao, Y., Jin, H., Liu, B., Herrmann, M., Sun, Z., Wang, Y., 2015. Holocene climate change on the northeastern Tibetan Plateau inferred from mountain-slope pollen and non-pollen palynomorphs. *Rev. Palaeobot. Palynol.* 221, 22–31.
- Mischke, S., Weynell, M., Zhang, C., Wiechert, U., 2013. Spatial variability of  $^{14}\text{C}$  reservoir effects in Tibetan Plateau lakes. *Quat. Int.* 313–314, 147–155.
- Morrill, C., Overpeck, J.T., Cole, J.E., 2003. A synthesis of abrupt changes in the Asian summer monsoon since the last deglaciation. *Holocene.* 13, 465–476.
- Ni, Z., Jones, R., Zhang, E., Chang, J., Shulmeister, J., Sun, W., Wang, Y., Ning, D., 2019. Contrasting effects of winter and summer climate on Holocene montane vegetation belts evolution in southeastern Qinghai-Tibetan Plateau, China. *Paleogeogr. Paleoclimatol. Paleoecol.* 533, 109232.
- Ni, J., Yu, G., Harrison, S.P., Prentice, I.C., 2010. Palaeovegetation in China during the late Quaternary: Biome reconstructions based on a global scheme of plant functional types. *Paleogeogr. Paleoclimatol. Paleoecol.* 289, 44–61.
- Nishimura, M., Matsunaka, T., Morita, Y., Watanabe, T., Nakamura, T., Zhu, L., Nara, F. W., Imai, A., Izutsu, Y., Hasuike, K., 2014. Palaeoclimatic changes on the southern Tibetan Plateau over the past 19,000 years recorded in Lake Pumoyung Co, and their implications for the southwest monsoon evolution. *Paleogeogr. Paleoclimatol. Paleoecol.* 396, 75–92.
- Overpeck, J., Anderson, D., Trumbore, S., Prell, W., 1996. The southwest Indian Monsoon over the last 18000 years. *Clim. Dyn.* 12, 213–225.
- Qin, F., Zhao, Y., Li, Q., Cai, M., 2015. Modern pollen assemblages from surface lake sediments in northwestern China and their importance as indicators of vegetation and climate. *Sci. China Earth Sci.* 58, 1643–1655.
- Qiu, J., 2008. China: the third pole. *Nature.* 454, 393–396.
- Reimer, P.J., Bard, E., Bayliss, A., Beck, J.W., Blackwell, P.G., Ramsey, C.B., Buck, C.E., Cheng, H., Edwards, R.L., Friedrich, M., Grootes, P.M., Guilderson, T.P., Hafldadson, H., Hajdas, I., Hatté, C., Heaton, T.J., Hoffmann, D.L., Hogg, A.G., Haghén, K.A., Kaiser, K.F., Kromer, B., Manning, S.W., Niu, M., Reimer, R.W., Richards, D.A., Scott, E.M., Southon, J.R., Staff, R.A., Turney, C.S.M., van der Plicht, J., 2013. IntCal13 and Marine13 radiocarbon age calibration curves 0–50,000 years cal BP. *Radiocarbon.* 55, 1869–1887.
- Ren, G., Beug, H.J., 1999. The mapping of Holocene pollen data in China. *Veg. Hist. Archaeobot.* 8, 231–232.
- Ren, G., Beug, H.J., 2002. Mapping Holocene pollen data and vegetation of China. *Quat. Sci. Rev.* 21, 1395–1422.
- Ren, G., Zhang, L., 1998. A preliminary mapped summary of Holocene pollen data for Northeast China. *Quat. Sci. Rev.* 17, 669–688.
- Schlutz, F., Lehmkuhl, F., 2009. Holocene climatic change and the nomadic Anthropocene in Eastern Tibet: palynological and geomorphological results from the Nianbaoyeze Mountains. *Quat. Sci. Rev.* 28, 1449–1471.
- Schwendemann, A.B., Wang, G., Mertz, M.L., McWilliams, R.T., Thatcher, S.L., Osborn, J. M., 2007. Aerodynamics of saccate pollen and its implications for wind pollination. *Am. J. Bot.* 94, 1371–1381.

- Shan, F., Kong, Z., Du, N., 1996. Palaeovegetation and environmental changes. In: Li, B. (Ed.), *Physical Environment of Hoh Xil Region, Qinghai*. Science Press, Beijing, pp. 197–206 (in Chinese).
- Shang, X., Li, X., An, Z., Ming, J., Zhang, H., 2009. Modern pollen rain in the Lake Qinghai basin, China. *Sci. China Ser. D* 52, 1510–1519.
- Shen, C., 2003. Millennial-Scale Variations and Centennial-Scale Events in the Southwest Asian Monsoon: Pollen Evidence from Tibet. Louisiana State University, PhD Dissertation.
- Shen, C., Liu, K., Morrill, C., Overpeck, J.T., Peng, J., Tang, L., 2008. Ecotone shift and major droughts during the mid-late Holocene in the central Tibetan Plateau. *Ecology* 89, 1079–1088.
- Shen, C., Liu, K., Tang, L., Overpeck, J.T., 2006. Quantitative relationships between modern pollen rain and climate in the Tibetan Plateau. *Rev. Palaeobot. Palynol.* 140, 61–77.
- Shen, C., Tang, L., Wang, S., 1996. Vegetation and climate during the last 22 000 years in Zoige region. *Acta Micropalaeontologica Sinica* 4, 401–406 (in Chinese with English abstract).
- Sinha, A., Cannariato, K.G., Stott, L.D., Li, H., You, C., Cheng, H., Edwards, R.L., Singh, I. B., 2005. Variability of Southwest Indian summer monsoon precipitation during the boiling-Ållerød. *Geology* 33, 813–816.
- Sirocko, F., Sarnthein, M., Erlenkeuser, H., Lange, H., Arnold, M., Duplessy, J.C., 1993. Century-scale events in monsoonal climate over the past 24,000 years. *Nature* 364, 322–324.
- Sun, H., 1999. *The National Physical Atlas of China*. China Cartographic Publishing House, Beijing (in Chinese).
- Sun, X., Du, N., Chen, Y., Gu, Z., Liu, J., Yuan, B., 1993. Holocene palynological records in Lake Selincuo, northern Xizang. *Acta Bot. Sin.* 35, 943–950 (in Chinese with English abstract).
- Sun, X., Zhao, Y., Li, Q., 2017. Holocene peatland development and vegetation changes in the Zoige Basin, eastern Tibetan Plateau. *Sci. China-Earth Sci.* 60, 1826–1837.
- Tan, L., Cai, Y., Cheng, H., Edwards, L.R., Lan, J., Zhang, H., Li, D., Ma, L., Zhao, P., Gao, Y., 2018. High resolution monsoon precipitation changes on southeastern Tibetan Plateau over the past 2300 years. *Quat. Sci. Rev.* 195, 122–132.
- Tang, H.S., 1999. Discussing the paleolithic and microlith on the Tibetan Plateau. *Archaeology* 5, 44–54.
- Tang, L., Shen, C., 1996. Holocene pollen records of the Qinghai-Xizang Plateau. *Acta Micropalaeontologica Sinica* 4, 407–422 (in Chinese with English abstract).
- Tang, L., Shen, C., Liu, K., Overpeck, J.T., 1999. New high-resolution pollen records from two lakes in Xizang (Tibet). *J. Integr. Plant Biol.* 41, 896–902 (in Chinese with English abstract).
- Thompson, L.G., Yao, T., Davis, M.E., Henderson, K.A., Mosley-Thompson, E., Lin, P., Beer, J., Synal, H.A., Cole-Dai, J., Bolzan, J.F., 1997. Tropical climate instability: the last Glacial cycle from a Qinghai-Tibetan ice core. *Science* 276, 1821–1825.
- Wang, M., 1987. The spore-pollen groups of peatlands on Ruergai Plateau and paleobotany and paleoclimate. *Sci. Geogr. Sin.* 2, 147–155 (in Chinese with English abstract).
- Wang, Y., Bekeschus, B., Handorf, D., Liu, X., Dallmeyer, A., Herzschuh, U., 2017. Coherent tropical-subtropical Holocene see-saw moisture patterns in the Eastern Hemisphere monsoon systems. *Quat. Sci. Rev.* 169, 231–242.
- Wang, Y., Cheng, H., Edwards, R.L., He, Y., Kong, X., An, Z., Wu, J., Kelly, M.J., Dykoski, C.A., Li, X., 2005. The Holocene Asian monsoon: Links to solar changes and north Atlantic climate. *Science* 308, 854–857.
- Wang, Y., Herzschuh, U., Shumilovskikh, L.S., Mischke, S., Birks, H.J.B., Wischniewski, J., Boehner, J., Schluetz, F., Lehmkühl, F., Diekmann, B., Wuennemann, B., Zhang, C., 2014. Quantitative reconstruction of precipitation changes on the NE Tibetan Plateau since the last Glacial maximum-extending the concept of pollen source area to pollen-based climate reconstructions from large lakes. *Clim. Past* 10, 21–39.
- Wang, W., Li, C., Shu, J., Chen, W., 2019. Changes of vegetation in southern China. *Sci. China-Earth Sci.* 62, 1316–1328.
- Wang, Y., Liu, X., Herzschuh, U., 2010. Asynchronous evolution of the Indian and East Asian Summer Monsoon indicated by Holocene moisture patterns in monsoonal central Asia. *Earth-Sci. Rev.* 103, 135–153.
- Wang, Y., Liu, X., Herzschuh, U., Yang, X., Birks, H.J.B., Zhang, E., Tong, G., 2012. Temporally changing drivers for late-Holocene vegetation changes on the northern Tibetan Plateau. *Paleogeogr. Paleoclimatol. Paleoecol.* 353–355, 10–20.
- Wang, Y., Shen, J., Wang, Y., Liu, X., Herzschuh, U., 2020. Abrupt mid-Holocene decline in the Indian summer monsoon caused by tropical Indian Ocean cooling. *Clim. Dyn.* 55, 1961–1977.
- Wang, W., Wang, Q., Li, S., Wang, G., 2006. Distribution and species diversity of plant communities along transect on the northeastern Tibetan Plateau. *Biodivers. Conserv.* 15, 1811–1828.
- Wang, P., Xia, Y., Wang, M., 1981. The study on the spore-pollen groups and the evolution of the natural environment of south Xizang Plateau in the peat of the Holocene. *Sci. Geogr. Sin.* 1, 144–152 (in Chinese with English abstract).
- Wang, P., Xia, Y., Wang, M., 1988. An approach to the spore-pollen assemblages of peat in the Holocene and the evolution of natural environment in southern Xizang. In: Huang, X. (Ed.), *Study of Mire in China*. Science Press, Beijing, pp. 257–265 (in Chinese).
- Wei, H., Ma, H., Zhuo, Z., Pan, A., Huang, K., 2011. Modern pollen assemblages of surface samples and their relationships to vegetation and climate in the northeastern Qinghai-Tibetan Plateau. *China. Rev. Palaeobot. Palynol.* 163, 237–246.
- Wei, H., Zhao, Y., 2016. Surface pollen and its relationships with modern vegetation and climate in the Tianshan Mountains, northwestern China. *Veget. Hist. Archaeobot.* 25, 19–27.
- Wischniewski, J., Mischke, S., Wang, Y., Herzschuh, U., 2011. Reconstructing climate variability on the northeastern Tibetan Plateau since the last late Glacial—a multi-proxy, dual-site approach comparing terrestrial and aquatic signals. *Quat. Sci. Rev.* 30, 82–97.
- Wu, Z., 1995. *The Vegetation of China*. Science Press, Beijing (in Chinese).
- Wu, Y., Xiao, J., 1996. A pollen record during the past 30000 years from the Zabuye Lake, Tibet. *Marine Geol. Quat. Geol.* 03, 115–122 (in Chinese with English abstract).
- Yan, G., Wang, F., Shi, G., Li, S., 1999. Palynological and stable isotopic study of palaeoenvironmental changes on the northeastern Tibetan Plateau in the last 30,000 years. *Paleogeogr. Paleoclimatol. Paleoecol.* 153, 147–159.
- Yang, B., Qin, C., Wang, J., He, M., Melvin, T.M., Osborn, T.J., Briffa, K.R., 2014. A 3,500-year tree-ring record of annual precipitation on the northeastern Tibetan Plateau. *Proc. Natl. Acad. Sci. U. S. A.* 111, 2903–2908.
- Yu, G., Tang, L., Yang, X., Ke, X., Harrison, S.P., 2001. Modern pollen samples from alpine vegetation on the Tibetan Plateau. *Glob. Ecol. Biogeogr.* 10, 503–519.
- Zanon, M., Davis, B.A.S., Marquer, L., Brewer, S., Kaplan, J.O., 2018. European forest cover during the past 12,000 years: a palynological reconstruction based on modern analogs and remote sensing. *Front. Plant Sci.* 9, 253.
- Zhang, Y., Duo, L., Pang, Y., Felde, V.A., Birks, H.H., Birks, H.J.B., 2018. Modern pollen assemblages and their relationships to vegetation and climate in the Lhasa Valley, Tibetan Plateau, China. *Quat. Int.* 467, 210–221.
- Zhang, Y., Kong, Z., Zhang, Q., Yang, Z., 2015. Holocene climate events inferred from modern and fossil pollen records in Butuo Lake, Eastern Qinghai-Tibetan Plateau. *Clim. Chang.* 133, 223–235.
- Zhang, Z., Li, C., 2017. Distributional patterns of anemophilous tree pollen indicating the pathways of Indian monsoon through Qinghai Tibetan Plateau. *J. Palaeogeogr.* 6, 352–358.
- Zhang, E., Wang, Y., Sun, W., Shen, J., 2016. Holocene Asian monsoon evolution revealed by a pollen record from an alpine lake on the southeastern margin of the Qinghai-Tibetan Plateau, China. *Clim. Past* 12, 415–427.
- Zhao, K., Li, X., 2013. Modern pollen and vegetation relationships in the Yili Basin, Xinjiang, NW China. *Chin. Sci. Bull.* 58, 4133–4142.
- Zhao, Y., Li, F., Hou, Y., Sun, J., Zhao, W., Tang, Y., Li, H., 2012b. Surface pollen and its relationships with modern vegetation and climate on the Loess Plateau and surrounding deserts in China. *Rev. Palaeobot. Palynol.* 181, 47–53.
- Zhao, Y., Liu, H., Li, F., Huang, X., Sun, J., Zhao, W., Herzschuh, U., Tang, Y., 2012a. Application and limitations of the *Artemisia/Chenopodiaceae* pollen ratio in arid and semi-arid China. *Holocene* 22, 1385–1392.
- Zhao, Z., Liu, A., Peng, W., 2007a. Holocene environmental changes of northern Qinghai-Tibetan Plateau based on spore-pollen analysis. *Arid Land Geography* 03, 381–391 (in Chinese with English abstract).
- Zhao, Y., Miao, Y., Fang, Y., Li, Q., Lei, Y., Chen, X., Dong, W., An, C., 2021. Investigation of factors affecting surface pollen assemblages in the Balikun basin, central Asia: implications for palaeoenvironmental reconstructions. *Ecol. Indic.* 123, 107332.
- Zhao, Y., Yu, Z., Chen, F., Ito, E., Zhao, C., 2007b. Holocene vegetation and climate history at Hurlig Lake in the Qaidam Basin, northwest China. *Rev. Palaeobot. Palynol.* 145, 275–288.
- Zhao, Y., Yu, Z., Zhao, W., 2011. Holocene vegetation and climate histories in the eastern Tibetan Plateau: controls by insolation-driven temperature or monsoon-derived precipitation changes? *Quat. Sci. Rev.* 30, 1173–1184.
- Zhao, P., Zhou, X., Chen, J., Liu, G., Nan, S., 2019. Global climate effects of summer Tibetan Plateau. *Sci. Bull.* 64, 1–3.
- Zhou, X.M., 2001. *China's Kobresia Meadows*. Science Press, Beijing (in Chinese).
- Zhou, L., Gui, L.P., Hai, T., 2008. Pollen indicators of human activity. *Chin. Sci. Bull.* 53, 1281–1293.